Na^+/H^+ transporters of the halophyte *Mesembryanthemum crystallinum* L.

Vom Fachbereich Biologie der Technischen Universität Darmstadt
zur Erlangung des akademischem Grades eines
Doctor Rerum Naturalium
genehmigte Dissertation

CRISTIAN COSENTINO

aus Milano (Italien)

Berichterstatter: PD Dr. Ulrike Homann
Mitberichterstatter: Prof. Dr. Gerhard Thiel

Tag der Einreichung: 16 Juni 2008
Tag der mündlichen Prüfung: 31 Juli 2008

Darmstadt, 2008
D17

To my family

To the sweet and wonderful Floriana who lived and faced the difficulties that this longtime experience carried into our love

Special thanks to Elke and Ulrike for the great help, confidence and smile they brought to me during the work

To Gerhard, who always addressed me to the right question to get the right result. Unforgettable the beer breaks and the travels by car with you!

All the people I have worked with: Brigitte, the worker, the cyclist, the runner, the climber, the skier, the great ping-pong player…she's incredible!; Adam, my yeast guru; Dirk, the great thisch fussball player; Jörg, the real football player; Henrik, the german-italian friend; Jenny the Biker, discoverer of the magic SURE E. coli cells; fac totum Karl; Vera, the BY2 cells' mother, Andi, Hi-jea and Christian the good drinkers, Martin the Smoker; and again Mirja, Michael, Melanie, Muriel, Aline, Uta, Claudia, Alice, Barbara, Sylvia and Silvia, Regina and Detlef, Manuela, Timo, Julia… for the nice time I have spent with you.

All the Darmastädter citizens I've eaten, drunk and played WC3 with: Ugolo, Simon, l'Albertide, la Romina, Uncle Bob, Zilvia, Woytinsky, Sbollaus and Cinzia

See you all again!

Milano 15.6.2008
Cristian Cosentino

1 Summary

The aim of this work was to understand the mechanisms of Na^+ accumulation in the halophyte *Mesembryanthemum crystallinum* L. during NaCl induced transition from C3 photosynthesis to crassulacean acid metabolism (CAM). Under high salinity *M. crystallinum* is a strong salt includer accumulating high amounts of Na^+ in leaves. To understand the mechanisms of Na^+ accumulation during NaCl adaptation Na^+/H^+ antiporters from leaves of *M. crystallinum* were cloned by RACE PCR. *In silico* analysis identified the five cloned antiporters as belonging to three different families of exchangers: NhaP/SOS1 family, represented by McSOS1; IT/NhaD, represented by McNhaD: IC-NHE/NHX, with McNHX1 and McNHX3 belonging to the vacuolar class I and McNHX2 to the endomembrane class II. McSOS1, McNhaD and McNHX1 are homologous to the Na^+/H^+ antiporters AtSOS1, AtNHX1-2 and AtNHD1 of *Arabidopsis thaliana*, which are located at the plasma membrane, tonoplast and plastidial membrane, respectively. Functional complementation tests in *Saccharomyces cerevisiae* revealed that McSOS1 and McNhaD can complement the Na^+ sensitivity of a yeast mutant strain (*ena1-4 nha1 nhx1*). Out of the three cloned antiporters of the IC-NHE/NHX family only McHX1 was able to restore resistance to Hygromycin B in the yeast mutant strain *nhx1* implying that only this antiporter functions at the vacuolar membrane.

Real-time PCR analysis demonstrated that the expression level of McSOS1, McNhaD and McNHX1 increased under salt stress. This increase in expression level correlated with the accumulation of sodium in leaves suggesting a physiological role for the antiporters in Na^+ compartmentation during adaptation to high salinity. In particular, analysis of salt accumulation on the cellular level revealed a high Na^+ content not only in vacuoles but also in chloroplasts. Together with the observation that the cloned antiporter McNhaD is localized to the plastidial membrane this points to a hitherto unknown pathway of Na^+ transport out of the cytosol. The integrated function of the Na^+/H^+ antiporter localized to the plasma membrane (McSOS1), the tonoplast (McNHX1) and the chloroplast membrane (McNhaD) will allow an immediate detoxification of the cytoplasm from Na^+.

2 Zusammenfassung

Ziel der vorliegenden Arbeit war die Untersuchung von Mechanismen, die an der Na^+-Akkumulation in der Halophyte *Mesembryanthemum crystallinum L.* während der NaCl induzierten Umstellung von C3-Photosynthese zum Crassulaceen-Säure-Metabolismus (CAM). Unter hoher Salzbelastung reichert *M. crystallinum* große Mengen an Na^+ in den Blättern an. Um den Mechanismus der Na^+-Akkumulation während der Salzanpassung zu verstehen wurden Na^+/H^+-Antiporter aus Blättern von *M. crystallinum* mittels RACE PCR kloniert. Die *in silico* Analyse der fünf klonierten Antiporter erlaubte die Zuordnung der Transportproteine zu drei verschiedenen Proteinfamilien: McSOS1 gehört zur NhaP/SOS1-Familie; McNhaD ist ein Transporter der IT/NhaD-Familie; McNHX1 (vakuoläre Membranen, Klasse I), McNHX2 (endosomale Membranen, Klasse II) und McNHX3 (vakuoläre Membranen, Klasse I) gehören zur IC-NHE/NHX-Familie. McSOS1, McNhad und McNhx1 sind homolog zu den Na^+/H^+ Antiportern AtSOS1, AtNhx1-2 und AtNHD1 in *Arabidopsis thaliana*, die an der Plasmamembran, am Tonoplasten und an der plastidären Membran lokalisiert sind. Funktionale Komplementationsexperimente mit *Saccaromyces cerevisiae* zeigen, dass McSOS1 und McNhaD die Na^+ Sensitivität der Hefemutante *ena1-4 nha1 nhx1* komplementieren können. Von den drei klonierten Antiportern der IC-NHE/NHX Familie konnte nur McHX1 die Hygromycin B-Resistenz in der Hefemutante *nhx1* wieder herstellen. Dies legt nahe, dass nur dieser Antiporter eine Funktion an der vakuolären Membran einnimmt.

Real-time PCR Analysen zeigten, dass die Expression von McSOS1, McNhaD und McNHX1 unter Salzstress ansteigt. Dieser Anstieg war mit der Akkumulation von Salz in Blätter korreliert und deutet auf eine physiologische Rolle dieser Antiporter in der Na+-Kompartimentierung während der Anpassung an hohe Na+-Konzentrationen hin. Die Analyse der Salzakkumulation auf zellulärer Ebene zeigt eine hohe Salzkonzentration nicht nur in Vakuolen, sondern auch in Chloroplasten. Die hohe Na+-Konzentration in Chloroplasten und die Lokalisation des klonierten Antiporters McNhaD an einer der plastidären Membranen weißt auf einen bisher unbekannten Weg für den Na+-Export aus dem Cytosol hin. Das Zusammenspiel der Na+/H+ Antiporter an der Plasmamembran (McSOS1), am Tonoplasten (McNHX1) und an der Chloroplastenmembran (McNhaD) gewährleistet eine schnelle Na+-Detoxifizierung des Cytosols.

3 Introduction

3.1 The present problem of soil salinization

It is estimated that about 15% of the total land area of the world has been degraded by soil erosion and physical and chemical degradation including soil salinization (Wild, 2003). Salinization is the accumulation of water-soluble salts in the soil. The total global area of salt-affected soils including saline and sodic soils was estimated in 2000 to be as large as about 831 million hectares extending over all the continents (Rengasamy, 2006). Among the various sources of soil salinity irrigation combined with poor drainage is the most serious because it represents losses of once productive agricultural land. Soil salinization severely limits agricultural productivity because concentrations as low as 25 mM NaCl are not tolerated by many plants and concentrations of 150 mM NaCl are highly toxic for most crop plants (Golldack, 2003). Na^+ specific damage is associated with the accumulation of this ion in leaf tissues and results in necrosis of older leaves. Consequently growth and yield reductions occur as a result of the shortening of the lifetime of individual leaves (Tester and Davenport, 2003). Instead at metabolic level the toxicity of Na^+ is largely a result of its ability to compete with K^+ for binding sites essential for cellular function.

Plants having the genetic potential to grow on saline soils are halophytes. These plants naturally grow under high salinity and are therefore salt tolerant. Whereas glycophytes are severely inhibited or even killed by 100-200 mM NaCl halophytes may tolerate elevated concentrations up to 500 mM NaCl. *Atriplex vesicaria* tolerates 700 mM NaCl while *Salicornia europaea* remains alive in more than 1 M NaCl (Zhu, 2007). Measurements of ion contents in plants treated with salt revealed that halophytes accumulate salts whereas glycophytes tend to exclude the salts. Halophytes might be divided into salt avoiders and salt includers. The second-ones are often succulent plants. Considering that halophytes often grow under very high salinity, it is not surprising that they have evolved mechanisms to accumulate ions in order to increase cell osmotic potential. This osmotic adjustment is necessary because the plants have to continue to extract water from the salty soil solution in order to meet the transpirational demand of their leaves. More than 80% of the accumulated ions in halophytes are carried in the transpirational stream of the xylem to the leaves. Some halophytes have also evolved specialized cells in the leaves and stems to remove the salts out of the plants.

3.2 Mechanisms of salt tolerance in plants

The maintenance of intracellular ion homeostasis is a fundamental concept in the physiology of living cells. Proper regulation of ion flux is necessary for cells to keep the concentrations of toxic ions low and to accumulate essential ions. Moreover, plants need to maintain internal water potential below that of the soil to maintain turgor and water uptake for growth. In typical physiological conditions plants maintain a low Na^+/K^+ ratio in their cytosol with relatively high K^+ (100–200 mM) and low Na^+ concentrations (1–10 mM) (Higinbotham, 1973). This ratio is important because K^+ as the most abundant cellular cation plays a critical role in maintaining an appropriate osmotic pressure for cell turgor regulation, membrane potential and cytosolic enzyme activities.

Under sodium stress the maintenance of K^+ and Na^+ homeostasis becomes even more crucial. Given the negative electrical membrane potential at the plasma membrane (ca. -120 to -300 mV) any rise in extra cellular Na^+ concentrations will establish a large electrical driving force for uptake of Na^+ into the cytosol. Once Na^+ ions enter the cytoplasm they inhibit the activity of many enzymes because of their similar chemical nature to K^+ ions. Na^+ specific damage is associated with the accumulation of Na^+ in leaf tissues and results in necrosis of older leaves, starting at the tips and margins and working back through the leaf; growth and yield reduction occur as a result of the shortening of the lifetime of individual leaves (Tester and Davenport, 2003). The cellular toxicity of Na^+ causes another type of osmotic problem. A major consequence of high external Na^+ concentration is the loss of intracellular water, since plants need to maintain internal water potential below that of the soil in order to keep turgor and water uptake for growth. This requires either increase of internal Na^+ accumulation or synthesis of compatible solutes with an osmolyte function such as sugars, betaine, proline and glycine.

Mechanisms to minimize damage from high Na^+ concentration include: reduction of the entry and increase of the efflux of Na^+ from the cell; increase of the intracellular compartmentation or allocation to particular tissues or cells (e.g. older leaves or trichomes); secretion of Na^+ onto the surface of leaves; decreasing of the loading of xylem. In general plants respond to Na^+ stress either as individual cells or synergistically as a whole organism by the control of long-distance transport and the site of Na^+ accumulation within the plant. The relative importance of these two mechanisms probably varies within species and conditions (Tester and Davenport, 2003).

Salt stress adaptation is also associated with changes in gene expression. Early genes are induced within minutes of stress signal perception and are often transiently expressed. This gene expression in turn may participate in the generation of hormones like ABA, salicylic acid and ethylene that amplify the initial signal and initiate a second round of signaling pathways (Mahajan and Tuteja, 2005).

Saccharomyces cerevisiae has been serving as a model system for studies of the molecular responses of salt adaptation not only in fungi but also in plants due to similarities in the regulation of osmotic and ion homeostasis. Yeast regulates the cytoplasmic K^+/Na^+ ratio by excluding Na^+ from cells and by accumulation the cation in pre-vacuolar compartments and vacuoles. The export of Na^+ from yeast cells is mediated by the Na^+-ATPase whereas the Na^+/H^+ antiporters mediate the extrusion of Na^+ from the cytosol to the vacuolar compartment (Nass *et al.*, 1997). In addition to Na^+ detoxification the vacuolar Na^+/H^+ antiporter serves other functions in yeast such as the participation in the generation of an osmotic driving force for passive water uptake via aquaporins (Nass *et al.*, 1998).

The cytosolic enzymes of halophytes are just as sensitive to Na^+ as enzymes of glycophytes. This implies that their successful salt adaptation depends on maintenance of cytoplasmic ion homeostasis with discrimination of K^+ over Na^+. Unlike animal and yeast, plant cells do not have Na^+-ATPases or Na^+/K^+-ATPases for transport of Na^+ out of the cytosol. Instead plants have to create a proton motive force across the plasma membrane and tonoplast that drives transport of Na^+ and other ions and metabolites. At the tonoplast the H^+ motive force is created by the vacuolar H^+-ATPases (V-ATPase) and the H^+-pyrophosphatases (V-PPase) (Hasegawa *et al.*, 2000). The importance of the establishment of a proton motive force during salt stress is underlined by the salt-dependent activation of vacuolar V-ATPases (Ratajczak et al., 1994) and the proton gradient has been shown to be correlated with vacuolar Na^+/H^+ antiport activity (Barkla *et al.*, 1995; Binzel and Ratajczak, 2001). This seems to be a specific response mechanism in halophytes that is missing in glycophytes such as *A. thaliana* (Kluge *et al.*, 1999). Moreover, vacuolar V-PPase shows increased protein amount in the halophyte *Suaeda salsa* (Wang *et al.*, 2001) reinforcing the H^+ driven Na^+ storage mechanism at least in some plants. However, Bremberger *et al.* (1988) and Rackel *et al.* (1994) measured a decrease of the V-PPase activity and protein amount for *M. crystallinum* under salt stress conditions (Rockel *et al.*, 1994).

Na^+ exhibits also a strong inhibitory effect on K^+ uptake by the root. Plants use both low- and high-affinity systems for K^+ uptake. Na^+ ions have a more damaging effect on the low-

affinity system which has high Na^+/K^+ selectivity. For that reason plants have to operate the more selective high-affinity K^+ uptake system in order to maintain adequate K^+ nutrition.
Finally, an important factor in the battle between Na^+ and K^+ ions is calcium. Increased calcium supply has a protective effect on plants under sodium stress. Calcium sustains potassium transport and Na^+/K^+ selectivity in sodium-challenged plants. Calcium may also directly suppress Na^+ import mediated by nonselective cation channels (Zhu, 2003).

3.3 Na^+/H^+ antiports for extrusion of Na^+ cations from the cytoplasm

Phylogenetic analysis of the completed Arabidopsis genome sequence has revealed the existence of a large family of putative cation/H^+ antiporters. Based on the electrochemical gradients of their relative ionic substrates most of these exchangers are thought to extrude cations from the cytosol to the outside across the plasma membrane or into intracellular compartments. Up to four phylogenetic subfamilies of cation/H^+ exchangers have been identified within the Arabidopsis genome that may exchange Ca^{++}, Na^+ and K^+ for H^+ (Mäser *et al.*, 2001).
The CaCA gene group of Ca^{++}/H^+ exchangers contains 11 members that have been named AtCAX1 to AtCAX11. A line of evidence indicate that CAX genes may play a central role in Ca^{++} and metal (Mn^{++} and Cd^{++}) sequestration into the vacuole but several members of this group still remain to be characterized (Pardo *et al.*, 2006).
The later groups (IT/NhaD, CPA1 and CPA2) are transporters specific for Na^+ and K^+/H^+ exchange. In Arabidopsis there are two members of the IT/NhaD group, AtNhaD1 and AtNhaD2 that have similarity to Na^+/H^+ antiporters previously found in bacteria, both of which remain uncharacterized (Pardo *et al.*, 2006).
The CPA1 group counts eight members in Arabidopsis and they can be divided into NHE/NHX and NhaP/SOS1 families that include the best characterized proteins, AtNHX1 and SOS1, catalyzing Na^+/H^+ exchange at the tonoplast and plasma membrane, respectively (Blumwald, 2000). On the basis of protein sequence similarity the NHE/NHX family can be classified in two major groups, the plasma membrane (PM-) and intra-cellular (IC-) subfamilies. The first is exclusively present in animal cells, whereas members of the second subfamily can be found in animals, plants and fungi with the exception of NHE8-like exchangers that are found only in animals. All plant NHX characterized to date are assigned to the IC-NHE/NHX subfamily. Since the high number of genes present in this subfamily IC-NHE/NHX can be further divided into Class I (AtNHX1-4) localized at the

vacuolar membrane and Class II (AtNHX5-6) localized at the endosomal compartments (Pardo *et al.*, 2006).

Finally the large CPA2 group has 33 members in Arabidopsis that include 28 CHX proteins thought to mediate cation/H^+ exchange and 5 homologues of the K^+/H^+ antiporter AtKEA1. Members of this group are just beginning to be characterized (Pardo *et al.*, 2006).

3.3.1 SOS1-type antiporter for cellular Na+ efflux

Little is known about how Na^+ is sensed in any cellular system. Theoretically Na^+ can be sensed either before or after entering the cell, or both. Extra-cellular Na^+ may be sensed by a membrane receptor whereas intracellular Na^+ may be sensed either by membrane proteins or by any of the many Na^+ sensitive enzymes in the cytoplasm.

Genetic analysis has shown that the maintenance of a low concentration of cytoplasmic Na^+ is a key player in sodium tolerance and it has been hypothesized that the plasma membrane Na^+/H^+ antiporter (SOS1) might function as a sensor for Na^+ (Zhu, 2002).

The first detectable response to Na^+ stress is a rise in the cytosolic free calcium concentration. This calcium signal serves as a second messenger that turns on the machinery for sodium export and K^+/Na^+ discrimination. In plant cells SOS3 has been identified as the sensor protein for this calcium signal because a loss-of-function mutation in this protein renders the *A. thaliana* plant overly sensitive to salt. SOS3 forms a complex with the serine/threonine protein kinase SOS2. Upon receiving the calcium signal the kinase complex is activated to phosphorylate target proteins such as SOS1. SOS1 was initially identified as a genetic locus required for salt tolerance in Arabidopsis (Wu *et al.*, 1996); subsequently the SOS1 gene has been identified as encoding for a plasma membrane Na^+/H^+ antiporter (Shi *et al.*, 2000). This exchanger is responsible for removing Na^+ from the cells (Zhu, 2002) and it is essential for controlling long-distance Na^+ movement in plants (Shi et al., 2002b). Mutations in SOS1 inducing the loss of function render plants extremely sensitive to Na^+. The transcript level of SOS1 is up-regulated by NaCl stress but not by drought, cold or ABA (Shi *et al.*, 2000). The sodium extrusion activity of SOS1 finally depends on SOS3 and SOS2.

3.3.2 NHX-type antiporter for vacuolar Na^+ storage

An important mechanism in dealing with cytosolic Na^+ is to store it in the vacuolar compartment where it is not in contact with cytosolic enzymes. Vacuolar compartmentation of Na^+ is achieved by the action of Class I of Na^+/H^+ antiporters of IC-NHE/NHX subfamily that localize to the tonoplast. The first gene coding for a plant vacuolar Na^+/H^+

antiporter was isolated from *A. thaliana* by its homology to the yeast Na^+/H^+ exchanger NHX1 (Nass *et al.*, 1997; Apse *et al.*, 1999). *A. thaliana* plants over-expressing the AtNHX1 antiporter gained salt resistance to 200 mM NaCl, a concentration that severely damaged wild-type plants (Apse *et al.*, 1999). Vacuolar compartmentation of Na^+ is perhaps more important for halophytes that actively accumulate large amounts of this ion. The counter ions are typically chloride and malate. Vacuolar sequestration of Na^+ not only lowers Na^+ concentration in the cytoplasm but also contributes to osmotic adjustment to maintain water uptake from saline solutions.

In *A. thaliana*, the AtNHX family of Na^+/H^+ antiporters functions in internal Na^+ compartmentation (Blumwald, 2000). AtNHX1 and AtNHX2 are localized at the tonoplast and their transcript levels are up-regulated by ABA or osmotic stress (Yokoi *et al.*, 2002). Over-expression of AtNHX1 in various plants has been reported to enhance plant salt tolerance substantially (Dietz *et al.*, 2001). The protein kinase SOS2, responsible for activating the plasma membrane SOS1 antiporter has been found to be important for the activation of the vacuolar antiporters. Therefore the SOS pathway appears to regulate also the activity of vacuolar Na^+/H^+ antiporters (Zhu, 2003).

Osmotic stress also plays a role by activating the synthesis of abscisic acid (ABA) which can up-regulate the transcription of AtNHX1 (Shi *et al.*, 2002a). However, Na^+/H^+ antiport seems to be regulated through ABA-independent pathways in the halophyte *M. crystallinum* under salt stress suggesting a different cascade of mechanisms for the regulation of the Na^+ tolerance in this plant (Barkla *et al.*, 1999).

3.3.3 NhaD-type antiporter for chloroplast Na^+ storage

Organelles such as plastids and mitochondria may also accumulate some Na^+ and thus contribute to the overall subcellular compartmentation of Na^+ (Pardo *et al.*, 2006). Analysis of the genome sequences of Arabidopsis and rice has revealed that some of Na^+ antiport proteins belong to families with many members, as for the NHX-type, although for others such as SOS1 only one or at most two genes exist (Garciadeblàs *et al.*, 2007). The membranes in which plant transporters are expressed and the functions of each family member are currently being studied. However, very little is known about plant NhaD-type transporters. These transporters show sequence similarity with bacterial NhaD Na^+/H^+ antiporters that have been identified in *Vibrio parahaemolyticus* (Nozaki *et al.*, 1998) and *Vibrio cholerae* (Dzioba *et al.*, 2002). They mediate Na^+ and Li^+ effluxes and have been characterized as Na^+ and Li^+/H^+ antiporters. Although this function is shared with other bacterial

antiporters such as NhaA and NhaB (Padan *et al.*, 2001) which also exist in *V. cholerae* (Herz *et al.*, 2003) and *V. parahaemolyticus* (Kuroda *et al.*, 2005) NhaD is peculiar because homologous sequences have been found also in plants.

In plants NhaD transporters have been cloned and characterized in *Populus euphratica* (PeNhaD1; Ottow *et al.*, 2005) and *Physcomitrella patens* (PpNhaD1; Barrero-Gil *et al.*, 2007). Homology based analyses indicate that NhaD-types of transporters exist in several plant species, as in Arabidospis, and they localize in chloroplast membranes (Barrero-Gil *et al.*, 2007). Functional expression of PeNhaD1 and PpNhaD1 in a *nhaA nhaB E. coli* double mutant (EP432 strain) revealed that both antiporters are able to recover Na^+ and Li^+ toxicities.

3.4 The halophyte plant *Mesembryanthemum crystallinum* L.

In this study, investigation on the mechanism of Na^+ tolerance was carried out in *Mesembryanthemum crystallinum*. *M. crystallinum*, also termed common ice plant, is an annual halophyte belonging to the family of *Aizoaceae*, order *Caryophyllales*. This species is native to southern and eastern Africa (Winter, 1972); later it has been introduced to Western Australia, around the Mediterranean, along coasts of the western United States, Mexico, Chile and Caribbean (Adams *et al.*, 1998). In its native habitat, the plant germinates and becomes established after a short winter rainy season, followed by progressive drought stress in connection with increasing salinity as the season proceeds. Such conditions have resulted in the evolution of acclimatory processes which can be defined in terms of anatomical, physiological, biochemical and molecular processes. One of these processes is a developmentally programmed switch from C3 photosynthesis to crassulacean acid metabolism (CAM), an eco-physiological modification of photosynthetic carbon acquisition (Lüttge, 2004). The switch from C3 metabolism to CAM is accelerated by salinity and drought or high irradiance (Adams *et al.*, 1998; Broetto *et al.*, 2002). Depending on the strength of the stress and the developmental stage the shift of metabolism let the plant minimize water loss and survive long in the stressful dry period (Winter *et al.*, 1974; Lüttge, 1993; Bohnert and Cushman, 2000). In contrast to many facultative CAM plants in which induction is reversible, the induction of CAM in adult leaves of *M. crystallinum* is constitutive and coincides with the transition to mature growth (Adams *et al.*, 1998).

Since the metabolic switch can be induced by stressing the plant, *M. crystallinum* has became an important model for biochemical and physiologic studies of CAM. This metabolism is present in approximately 7% of vascular plant species. Its hallmark is a diurnal fluctuation of

carbon such that the initial fixation of CO_2 is accomplished by PEP carboxylase during the night when stomata are open. The fixed CO_2 is stored in vacuoles as malate, which is mobilized under light conditions behind closed stomata for final fixation by RUBISCO (Cushman and Bohnert, 1999; Lüttge, 2004). The CO_2 concentrating mechanism improves water use efficiency of CAM species up to five fold relative to C3 and C4 species and provides CAM plants with a competitive advantage in hot, dry climates (Nobel, 1996).

In *M. crystallinum* CAM can also be induced by NaCl treatment (Winter, 1973). The metabolic shift is accompanied by dramatic changes in gene expression which are synchronized with and responsible for new developmental patterns (Adams *at al.*, 1998; Cushman and Bohnert, 1999; Cushman *et al.*, 2008). Moreover, under these conditions, *M. crystallinum* proves to be a strong salt includer throughout its life (Heun *et al.*, 1991) and Na^+ accumulates in a gradient from roots (about 70 mM) to the growing shoot apices with the highest concentration stored in epidermal bladder cells (EBCs) (in excess of 1 M; Adams *et al.*, 1998). Recently a *M. crystallinum* mutant lacking epidermal bladder cells has been characterized and clearly showed that EBCs contribute to succulence by serving as a water storage reservoir and to salt tolerance by maintaining ion sequestration and homeostasis within photosynthetically active tissues (Agarie *et al.*, 2007).

Root growth is retarded under salinity indicating that water uptake by the root system is not essential for plant survival at the late developmental stages under heavy salinity (Kholodova *et al.*, 2002). Na^+ is effectively partitioned into vacuoles and its enhanced accumulation correlates with tonoplast Na^+/H^+ antiporter and V-ATPase activities (Barkla *et al.*, 1995; Chauhan *et al.*, 2000; Epimashko *et al.*, 2006). Finally Na^+ long distance transport seems to be based on Na^+/inositol symporters that function in conjunction with Na^+/ H^+ exchangers (Chauhan *et al.*, 2000; Bohnert and Cushman, 2000). Based on EST sequencing it is estimated that 10% of the total number of genes of *M. crystallinum* is responsive to salt stress most of which are coding for novel or functionally unknown proteins (Kore-eda *et al.*, 2004).

3.5 Aim of the work

The aim of this work was to understand the mechanisms of Na^+ accumulation in *M. crystallinum* during the NaCl induced switch from C3 photosynthesis to CAM.

In a first step RACE-PCR from mRNA of leaf mesophyll cells has been performed in order to clone Na^+/H^+ antiporters from salt treated *M. crystallinum* plants. The cloned antiporters have been characterized by functional complementation of *S. cerevisiae* and *E. coli*. Mutant strains. Localization studies of GFP fusion proteins have also been performed. To

determine the importance of the cloned antiporters the transcript levels of Na^+/H^+ antiporters in leaves and roots of plants under salt stress where analyzed by real-time PCR. In order to investigate the correlation between the expression characteristics of Na^+/H^+ antiporters and Na^+ accumulation in *M. crystallinum* plants some basic physiological parameters related to the adaptation of plants to high salinity and CAM induction have been monitored.

4 Materials and methods

4.1 Plant materials and growth conditions

Mesembryanthemum crystallinum plants from the collection of the Botanical Garden in Darmstadt were grown as previously reported by Broetto *et al.* (2002): plants were germinated in a 50% mixture of sand and soil (Type ED-73 DIN 11540–80 T), then transferred to soil only. Three weeks old plants were subsequently moved to a climate regulated growth chamber with a 12 h day-night light cycle. The irradiance at plant level of 300-350 μE m^{-2} s^{-1} (photosynthetically active radiation, λ=400–700 nm) was provided by QTI-AGRO 400 W daylight lamps (Philips). Temperature and relative humidity were 27°C and 60% during the day and 20°C and 80% during the night. At the age of 4 to 5 weeks the plants were stressed by irrigation with 400 mM NaCl over two weeks in order to induce CAM metabolism by salt stress.

4.2 RACE-PCR cloning

The Rapid Amplification of cDNA Ends (RACE) allows the amplification of an unknown end portion of a transcript using known information from the center of the transcript. It can be used to obtain the 5' end (5' RACE-PCR) or 3' end (3' RACE-PCR) of mRNA.

RNA from leaf and root tissues of *Mesembryanthemum crystallinum* harvested at different days of NaCl treatment (DNT) was purified with the RNeasy Plant minikit (Qiagen) and treated with RNase-free DNAase (Qiagen) accordingly to the manufacturer's protocol. From 2 to 3 μg of RNA were retro-transcribed with the SuperScript III RT enzyme (Invitrogen): 60 min at 50°C, followed by 15 min at 70°C for the inactivation of the enzyme, with 400 ng of oligo$(dT)_{17}$ or AP$(dT)_{17}$ (5'-GGCCACGCGTCGACTAGTACTTTTTTTTTTTTTTTT-3') primers for 3' RACE; 60 minutes at 55°C, followed by 15 minutes at 70°C, with 2 pmol of gene specific primers for 5' RACE. Finally 2 U of RNase H were added for 20 min at 37°C in order to avoid any double strand DNA-RNA.

In the case of 3' RACE amplification 0.2 μM_{fin} of a forward gene specific primer 1 (GS1f) versus 0.3-0.4 μM_{fin} of AP$(dT)_{17}$ or AP (5'-GGCCACGCGTCGACTAGTAC-3') were used in the first PCR. Instead for 5' RACE, a poly(dC) tail was polymerized at the 5' end of the cDNA with the terminal transferase TdT (NEB). The first PCR amplification was then conducted with 0.2 μM_{fin} of the forward AP$(dG)_{15}$ primer (5'-GGCCACGCGTCGACTAGTACGGGGGGGGGGGGGGG-3') versus 0.2 μM_{fin} of a

reverse gene specific primer 1 (GS1r). PCR were then diluted 1:400 and subjected to a nested PCR with 0.2 μM_{fin} of a GS2f, down-stream in respect of GS1f, versus 0.2 μM_{fin} of $AP(dT)_{17}$ or AP primer, in the case of 3' RACE; 0.2 μM_{fin} of a forward $AP(dG)_{15}$ primer versus 0.2 μM_{fin} of GS2r primer, up-stream in respect of GS1r, for 5' RACE. In the case of difficult amplifications a touch-down PCR protocol was performed: -0.2°C per cycle from T_m + 2°C to T_m – 4°C for 30-45 sec. Following nested PCRs with a GS3f primer, down-stream to GS1f and GS2f, versus $AP(dT)_{17}$ or AP (3' RACE) or GS3r, up-stream to GS1r and GS2r, versus $AP(dG)_{15}$, were eventually run in order to achieve a specific amplification band.

The RACE amplicons were inserted in the pCR4-TOPO vector (Invitrogen) and cloned into TOP 10 cells accordingly to the TOPO TA cloning system protocol (Invitrogen).

Transforming colonies were screened by colony PCR with 0.2 μM of T3 and T7 primers. A longer initial denaturation step (1 cycle at 95°C for 7 min) was added to the standard PCR amplification protocol in order to break the bacterial cells. Plasmids were subsequently extracted from the selected colonies and sent for sequencing to SeqLab (Göttingen, Germany).

4.3 Assembly of the sequences

The electropherograms obtained form each sequencing were filtered with Phred (http://bioinformatica.ucb.br/electro.html) and both low quality regions and vector sequence were removed by applying default parameters. A contig alignment of the RACE cloned sequences was performed with the ContigExpress utility provided within the VectorNTi package (Invitrogen) in order to create a consensus sequence for each gene. The 6 frames translation of the contig consensus let locate the final coding sequence of the genes. Multiple sequence alignments between the cloned Na^+/H^+ antiporters and heterologous proteins were performed with ClustalW (Higgins *et al.*, 1994; http://www.ebi.ac.uk/clustalw/index.html). Evolutionary distances were calculated by the neighbor joining method and the phylogenetic graph was computed using equal angle algorithm with equal-daylight and box-opening optimization in SplitsTree4 (Huson *et al.*, 2006). Protein identity values were calculated by pair-wise alignment with BLOSUM62 as similarity matrix. The sequences of the cloned genes were aligned by tblastx versus the EST repository data of *Mesembryanthemum crystallinum* at NCBI database, in order to find the best matching expressed sequence tags (EST).

4.4 Prediction of transmembrane domains and localization

The ARAMEMNON (http://aramemnon.botanik.uni-koeln.de/index.ep) database was taken as reference for looking up 18 different transmembrane domains (TMD) prediction programs (Schwacke *et al.*, 2003). The individual predictions for each protein were combined to a built-in average consensus where value 1 was assigned to the amino acids predicted as belonging to a TMD and value 0 to those not belonging to a TMD. All the programs were set-up with default parameters for plant proteins. The same ARAMEMNON database was also employed as reference for looking up 12 different programs for cellular localization prediction. Notice that not all programs perform predictions for all considered targets (chloroplast, mitochondrion, secretory pathways, other; Schwacke *et al.*, 2007; Table 1). Default settings for plant proteins were always used for each prediction algorithm.

Table 1. TMD and subcellular localization prediction programs employed in the analysis and referred to the ARAMEMNON database

TMD prediction		**Subcellular localization**	
PSORT II	THUMBUP_v1	ChloroP v1.1	PrediSi
ConPred II	TMap	iPSORT	Predotar
DAS-TMfilter	TmHMM_v2	MITOPRED	PredSL
HmmTop_v2	TMMOD	MitoProt II v1.0a4	SignalP v3.0_HMM
MemSat_v1.5	TmPred	PCLR v0.9	SignalP v3.0_NN
Phobius	TopPred_v2	PProwler v1.1	targetP v1.1
PredTmr_v1	PHDhtm		
SosuiG_v1.1	SPLIT		
SVMtm_v3	WaveTm		

4.5 Fluorescent imaging and GFP localization

The full length of the McNhaD gene was obtained by RT-PCR with specific primers carrying restriction sites: forward 5'-GCTAGCGGCCGCATGGCGTCTTCCCTCTCCTC-3 and reverse 5'-GTAGCGGCCGCATGAGCCAGAGATGAATGGAA-3' for McNhaD. The gene was inserted into a pUC19-GFP plasmid by NotI digestion, in order to have the GFP cassette at the C-terminus of the protein. The resulting plasmid was cloned in SURE *E. coli* strains in order to reduce the high recombination effects the plasmid exhibited in other strains. Confocal microscope analyses were carried out using a Leica TCS SP (Leica

Microsystems, Heidelberg, Germany) equipped with a 63× water immersion objective (plan apo, N.A. 1.2). Excitation levels were adjusted to cause minimal auto-fluorescent signal. For excitation, the 488 nm line of a 25 mW Ar/Kr ion laser and the TD 488/543/633 excitation beam splitter FW were used. In localization experiments GFP emission fluorescence was detected at 505 – 535 nm.

In experiments for Na^+ staining, ConoNa green (Invitrogen) fluorescence emission was detected with the confocal microscope at 505 – 540 nm and chlorophyll auto-fluorescence was allowed to be detected in the range 600 – 700 nn. Alternately, when a conventional transmission/epifluorescence microscope (Axiovert 100, Zeiss, Germany) was used, dye-loaded cells were excited with monochromatic light at 360 nm±1.2 nm. Fluorescence was separated from excitation light by a 495 nm dichromatic beam splitter and passed through a band pass filter with a cut-off at 525/550 nm for observation. Images were acquired with a digital camera (Power Shot G5, Canon) and analyzed by considering the red channel for pH staining and green channel for Na^+ staining. The images were furthermore background corrected by subtracting the grey from the respective channel considered. After cross-referencing with full color images intensities were counted for several cells and normalized to the maximum value. Finally their distribution was plotted as percentiles in a box chart. For Na^+ staining, 10 μM of CoroNa green dye were loaded into leaf cross-sections as 1:1 (v/v) mixture with 25% F-Pluronic 127, dissolved in 100 mM $CaCl_2$, 10 mM MES pH 6.1. The dye was loaded in 45' of incubation at 30°C, in the dark and under gentle mixing. For pH staining leaf cross sections were pre-incubated with 0.01% Neutral Red for 10 minutes at root temperature. Osmolarity was adjusted in both cases with sucrose. After loading leaf sections were washed in dye free buffer and cellular distribution of the dye was detected with the appropriate microscope. ImageJ (http://rsb.info.nih.gov/ij/index.html) was finally used for any further image processing.

4.6 Functional complementation in *Saccharomyces cerevisiae*

4.6.1 Yeast vector construction

The full length of the coding sequence was obtained by RT PCR with specific primers carrying restriction sites: forward 5'-CTAGGATCCAATGGCGTTTGATTTGAGTAATTTAG-3' and reverse 5'-CTAGCGGCCGCTTATGTACTCTCTGTCGAATGGTT-3', for McNHX1; forward 5'-CTAGGATCCAATGGAGGATCAGCTGATTTCTC-3' and reverse 5'-CTAGCGGCCGCTCAGTTGCGACTGAGATAGACT-3', for McNHX2; forward 5'-

CTAGGATCCAATGTCGATCTTGGGGTTTGATAC-3' and reverse 5'-CTAGCGGCCGCCTACTGCTCAATAATGGGATCTG-3', for McNHX3; forward 5'-CTAGAGCTCAATATGGCGTCTTCCCTCTCCTC-3 and reverse 5'-CTATCTAGATCATGAGCCAGAGATGAATGGAA-3', for McNhaD; forward 5'-CTAGGATCCATCATGGCGGCGTTGACTGATTT-3' and reverse 5'-CTAGCGGCCGCTCAAGGTGCGTGGCGGAACG-3', for McSOS1. All the genes were inserted into pYES2 yeast expression vector (Invitrogen) by BamHI/NotI digestion with the exception of McNhaD which was cloned by SacI/XbaI.

4.6.2 Yeast strains and expression

The *Saccharomyces cerevisiae* YDR456w deletion mutant (Mat a; his3Δ1; leu2Δ0; met15Δ0; ura3Δ0; YDR456w:kanMX4; Euroscarf Y04290) used for McNHX1, McNHX2 and McNHX3 functional complementation was isogenic to BY4741 (Mat a; his3Δ1; leu2Δ0; met15Δ0; ura3Δ0; Euroscarf Y00000) and was defective of the nhx1 gene. Indeed AB11c deletion mutant (Mat a; ade2-1; leu2-3; his3-11,15; trp1Δ2, ura3-1, ena1-4:HIS3, nhx1:TRP1, nha1:LEU2) was used for McSOS1 and McNhaD yeast complementation and was isogenic to W303 (Mat a; ura3-52; trp1Δ2; leu2-3,112; his3-11; ade2-1) (Maresova *et al.*, 2005). Yeast cells were grown in YPDA (1% yeast extract, 2% peptone, 2% dextrose, 5 μg/ml adenine sulphate), SD-Ura (0.67% yeast nitrogen base w/o amino acids, 2% dextrose, dropout supplements w/o Ura) or SD-Ura G/R (0.67% yeast nitrogen base w/o amino acids, 2% galactose, 1% raffinose, dropout supplements w/o Ura). Vectors were introduced into the respective strains using the lithium acetate method (Gietz *et al.*, 1995). Saturated yeast cultures in liquid SD–Ura medium were harvested, washed three times with distilled water and adjusted to final optic density measured at λ = 600 nm (OD_{600}) of 0.8. Ten-fold serial dilutions starting from OD_{600} = 0.8 were prepared for each strain and 5 μl of each dilution were spotted onto solid SD-Ura G/R, containing 100 μg/ml hygromycin B, and grown at 30°C for 2 days.

4.6.3 Na^+ determination in yeast cells

The internal Na^+ content of yeast cells was determined by flame spectrometry analysis (Gerätebau, Eppendorf, Hamburg, Germany). Yeast was grown on liquid SD-Ura G/R medium in order to induce gene expression, supplemented with 200 mM NaCl or 500 mM NaCl for experiments with W303 or B4741 genetic backgrounds, respectively. Saturated yeast cultures were harvested, washed three times and resuspended in 5 ml distilled water

and finally OD_{600} was detected. These cells were then boiled for 15 minutes in order to break membranes and release Na^+ from every internal compartment. After that the cell debris was centrifuged to the pellet and the cleaned supernatant was analyzed by flame spectrometer. Data were expressed as nmol $Na^+/10^8$ cells, 1 OD_{600} is equivalent to 2.2×10^7 cells.

4.7 Functional complementation in *Escherichia coli*

In order to clone McNhaD into the pQE60 *E. coli* expression plasmid (Promega) as mature protein, the sequence was analyzed by the ChloroP v1.1 program and a 35 aa signal peptide was detected. Standard PCR amplification was conducted with 0.2 μM_{fin} of the forward primer 5'-GCTAACATGTATGTCGCCGGCGACCGTTAACTC-3', carrying a PciI restriction site and inserting an ATG starting codon, and the reverse primer 5'-CTAAGATCTTCATGAGCCAGAGATGAATGGAA-3', carrying a BglII restriction site. Codons 36 to 577 were then cloned into pQE60 plasmid, digested NcoI and BglII. Transforming colonies were screened by colony PCR and the purified positive plasmids pQE60:McNhaD were sequenced in order to verify the integrity of the sequence.

Experiments of functional complementation were carried out using the *E. coli* double mutant strain EP432 (gently provided by T. Teichmann, University of Giessen, Germany), bearing deletions in *nhaA* and *nhaB* Na^+/H^+ antiporter genes. EP432 cells were grown on LBK medium (1% tryptone, 0.5 yeast extract, 1% KCl) supplemented with 34 μg/ml chloramphenicol. Chemical competent cells were transformed with pQE60 empty or pQE60:McNhaD transformant plasmid, then plated on LBK medium, supplemented with 100 μg/ml ampicillin and grown over night under aerobiotic conditions at 37°C. For the functional complementation tests fresh transformants colonies were pre-inoculated in liquid LBK medium supplemented with ampicillin as described above. Equal optic densities were inoculated in a new LBK media at different pH, depending on the experiment, supplemented with ampicillin. McNhaD expression was induced by 0.5 mM IPTG for 3 hours. After the induction phase, 5 mM LiCl or 200 mM NaCl were respectively added to the media as reported in Ottow *et al.* (2005). Optic density at 600 nm was detected every 2 hours up to the saturation of the cell growth.

Sensitivity to Li^+ was tested, together with Na^+ since the EP432 mutant may spontaneously convert to MH1 derivative which is Na^+ resistant, but it is stable with respect to Li^+ sensitivity (Harel-Bronstein et al., 1995). Data were analyzed by the logistic function [2] (see Material and Methods 2.13).

4.8 Real time PCR assay

A mixture of leaves or roots of three plants harvested at different days of NaCl treatment was prepared frozen in liquid nitrogen and stored at -80°C. Samples were collected every day at the end of the day-light cycle during 15 days of 400 mM NaCl treatment. Total RNA was then isolated, purified and 1-2 μg were retro-transcribed as previously described for RACE PCR cloning.

Primers were designed with Primer Express software (Applied Biosystems) and the ones within 50% GC content, 90-100 bp of amplicon length and 59°C of T_m were chosen for synthesis and HPLC purification (Biomers, Germany). The quality and specificity of the primers were carried out by checking 10, 20, 30 and 40 cycle-PCR amplification on a 1.2% agarose gel. Real time PCR assays were then performed on ABI PRISM® 7300 Real Time PCR System (Applied Biosystems) with SYBR® Green PCR Master Mix (Eppendorf). Data were acquired through the 7300 System SDS software v1.2 (Applied Biosystems) and Ct values were determined in Auto Ct mode. Standard curves were prepared with sequential dilutions in a range from 0.6 ng up to 150 ng of equivalent starting RNA. Slope values from fitting with R^2>0.999 were only considered. Standard curves and samples were run together on the sample plate. Actin was used as reference housekeeping gene. Here the primers used for the amplifications: forward 5'-AGGTCCTCTTCCAGCCTTCATT-3' and reverse 5'-CCTTCCTGATATCCACGTCACA-3', for actin; forward 5'-GATGCCTTGGACATCGAGAAGT-3' and reverse 5'-CATGAGCAGACCCAGCAATATG-3', for McNHX1; forward 5'-AGGTCCTCTTCCAGCCTTCATT-3' and reverse 5'-CCTTCCTGATATCCACGTCACA-3', for McNHX3; forward 5'-TTAGTCAGCACTCATCCTCTCCTG-3' and reverse 5'-GCGCACCTTGACAACTTCTTTC-3', for McSOS1; forward 5'-GGGATGTCACAACAACTATGCTCT-3' and reverse 5'-GGCACAGCCAAAGAAATAGCAG-3', for McNhaD. The detection of McNHX2 has failed even testing several couples of primers.

4.9 Malate, proline and osmolarity determination

The differences in leaf malate concentration at the beginning and the end of the light period were measured in the leaf cell sap of all samples as a basic indicator of CAM metabolism. Disks of leaf samples were collected and frozen in order to break cell walls, thawed and

centrifuged 5 min at 12000 × g. The supernatant was used for the enzymatically determination of malate concentration at the spectrometer (λ = 340 nm), accordingly to Möllering (1974). Leaf osmolarity was detected at the end of the light period by direct measurement at the osmometer (Osmomat 030, Gonotec, Berlin, Germany) of the cell sap of a mixture of three plants harvested at the same time. Proline was measured by the ninhydrin method of Bates (1973) and samples were from the same mixture used for leaf osmolarity determination. Briefly, approximately 500 mg of tissues were homogenized in 10 ml of 3% sulfosalicilic acid. 1 volume of filtered sample (#2 filter paper, Whatman) was added to 1 volume of ninhydrin acid solution and 1 volume of glacial acetic acid and the mixture was incubated in boiling water for 1 h in order to activate the colorimetric reaction. Two volumes of toluene were then added and the aqueous phase was recovered for proline determination at the spectrometer (λ = 520 nm) by using toluene as blank. Data of malate, osmolarity and proline determinations are mean values ± SD (n=3).

4.10 Ion determination by capillary electrophoresis

Plants were treated with 400 mM NaCl and harvested every day during the late light period. Each leaf or root sample is a mixture of three plants. An aliquot of these mixtures was weighted as fresh weight (FW) and burned to ashes at 540°C for 24h. After the determination of the dry weight samples were resuspended in 1 ml of 1N HCl and incubated over night at 37°C under gentle mixing. Finally, samples were centrifuged in order to pellet the ashes and the supernatant was recovered and subjected to capillary electrophoresis (CE) analysis. CE experiments were carried out with a Beckman P/ACE system 5510 (Beckman, Fullerton, USA) in a 100 μm capillary. Samples were pressure injected from microvials hydrodynamically for 30 s and separated for 4 min at 256 V/cm. Cations were detected indirectly by UV detection at 214 nm, For separation within the capillary Waters IonSelect™ low mobility cation electrolyte buffer (Waters) was used. Data are expressed as μmol/mg FW (n=3) ± SD and are analyzed by a logistic curve fitting [2] (see Material and Methods 2.13).

4.11 Chloroplasts isolation and chlorophyll determination essay

Plants were harvested every day during the early light period. Five g of leaves were homogenized with an electric mixer in 50 ml of H buffer (25 mM Hepes, pH 7.2 with Tris). Osmolarity was adjusted for each sample with sorbitol. The homogenized sample was

filtered trough a nylon membrane with 200 μm of pore size and centrifuged 1000g for 5 minutes in a swinging-bucket rotor. The pellet was then resuspended in 10 ml of the same H buffer and protoplasts were passed twice trough a 26 Gauge needle to brake the cells. Chloroplasts were further cleaned from the remaining protoplasts and cell debris by three times washing in 10 ml H buffer and centrifugation at 1000g for 3 minutes in a swinging-bucket rotor. Finally the pellet containing chloroplasts was resuspended in 5 ml of H buffer and subjected to flame spectrometry analysis.

Chlorophyll content was measured by the method of Arnon (1949), with some adaptation. Briefly, 10-50 μl of isolated chloroplasts were frozen in liquid nitrogen. Once warmed up, 80% acetone was added up to 1 ml of final volume. Samples were then incubated for 30 minutes in ice and darkness. Samples were centrifuged at maximum speed with minifuge, 500 μl or the supernatant were finally recovered and optic density was detected at 645 nm and 663 nm. The chlorophyll content was determined as following [1]:

[Equation 1] $$chlorophyll[\mu g/ml] = 20.2 \times E_{645} + 8.02 \times E_{663}$$

where E_{645} and E_{663} are the emissions detected at 645 and 663 nm, respectively.

4.12 Determination of the chloroplast Na^+ content

The Na^+ content of the isolated chloroplasts was determined by flame spectrometry analysis (Gerätebau, Eppendorf, Hamburg, Germany). The isolated chloroplasts were boiled for 15 minutes in order to release Na^+ from every internal compartment and then centrifuged to pellet the cell debris. The cleaned supernatant was recovered and analyzed at the flame spectrometer. The Na^+ content was determined by assuming that 100 μg of chlorophyll in *Mesembryanthemum crystallinum* is equivalent to 2-3 μl of chloroplast osmotic volume for C3 or CAM plants, respectively (Demming et al., 1983). Data were analyzed by a non-linear curve fitting [2] (see Material and Methods 2.13).

4.13 Interpolation of the data curves

Data were analyzed by a non-linear curve fitting using the Boltzman equation [2]:

[Equation 2] $$F(t) = \frac{A_{min} - A_{max}}{1 + (t/t_{1/2})^p} + A_{max}$$

Growth rates and ions, malate and proline accumulation curves where calculated by fitting the parameters determining the yielding A_{min} (starting cell density or concentration), A_{max} (final cell density or concentration), time when half of A_{max} was reached ($t_{1/2}$) and the growth exponent (p). Cell density for growth curve determination was measured as optic density at λ=600 nm.

4.14 Accession numbers

Sequence data from this work can be found in the EMBL/GenBank data libraries under the accession numbers: McNHX1 (CAN99589), McNHX2 (CAO01506), McNHX3 (CAP16138), McSOS1 (CAN99591) and McNhaD (CAN99590) for *Mesembryanthemum crystallinum*; AtNHX1 (NP_198067), AtNHX2 (Q56XP4), AtNHX3 (Q84WG1), AtNHX4 (AAM08405), AtNHX5 (Q8S396), AtNHX6 (AAM08407), AtSOS1 (NP_178307), AtNhaD1 (NP_566638) and AtNhaD2 (NP_175403) for *Arabidopsis thaliana*; RhNHX (BAD93487) for *Rosa hybrida*; PeNHX2 (ABD66754), PeNhaD (CAD91128) and PeSOS1 (ABF60872) for *Populus euphratica*; SjNHX (BAE95195) and SjSOS1 (BAE95196) for *Suaeda japonica*; SlNHX2 (CAC83608) and SlSOS1 (CAG30524) for *Solanum lycopersicum*; OsSOS1 (AAW33875) and OsNhaD (BAD17583) for *Oryza sativa*; ThSOS1 (ABN04857) and ThNHX1 (ABF48496) for *Thellungiella halophila*; TeSOS1 (AAQ91618) for *Triticum aestivum*; KfNHX (AAV73803) for *Kalidium foliatum*; TtNHX1 (AAQ08988) for *Tetragonia tetragonioides*; SeNHX1 (AY131235) for *Salicornia europaea*; AgNHX1 (AB038492) for *Atriplex gmelini*.

5 Results

5.1 Cloning of Na^+/H^+ antiporters from leaves of *Mesembryanthemum crystallinum*

The salt induced shift of *M. crystallinum* from C3 photosynthesis to CAM is associated with the exclusion of Na^+ from the cytosol via Na^+ efflux at the plasma membrane and/or Na^+ accumulation in intracellular compartments. Both processes require transport of Na^+ against an electrochemical gradient. This is most likely achieved by different Na^+/H^+ antiporters. In order to gain a deeper understanding of Na^+ transport and mechanisms involved in salt tolerance genes encoding for membrane Na^+/H^+ antiporters have been cloned from *M. crystallinum*.

The alignment of sequences coding for Na^+/H^+ antiporters of *A. thaliana* with the *M. crystallinum* EST repository revealed several putative Na^+/H^+ antiporters in the latter plant. The identified ESTs were used as basis for RACE-PCR cloning from total mRNA of leaf mesophyll cells of *M. crystallinum* plants exposed to high salinity. Using this approach 5 cDNA fragments have been obtained encoding internal fragments of different Na^+/H^+ antiporters. All fragments were extended towards the 3´ and 5´ end resulting in five full-length cDNAs named: McNhaD (AM746986), McSOS1 (AM746987), McNHX1 (AM746985), McNHX2 (AM748092) and McNHX3 (AM901401). Number of amino acids, predicted molecular weight and isoelectric point of the cloned antiporters are summarized in Table 2.

Table 2. Number of amino acids (aa), predicted molecular weight (MW) and isoelectric point (pI) of Na^+/H^+ antiporters cloned from *M. crystallinum* leaves and GeneBank accession numbers of the ESTs matching with the cloned antiporters (EST)

Gene	aa	MW	pI	EST
McNhaD	577	61.5	6.04	AW053497, BG269557, AI043527, AW053579
McSOS1	1115	127.3	5.97	BF479737, BE577626
McNHX1	549	60.8	6.44	AF279671, BE131520, BE131390
McNHX2	556	61.6	6.85	BE576906, BE036220, DY034828
McNHX3	526	58.1	5.59	AF279670, AA819990

Phylogenetic analysis reveals that the five cloned Na^+/H^+ antiporters belong to three different subfamilies (Fig. 1).

McNhaD groups into the IT/NhaD protein branch which was first found in bacteria and catalyzes Na^+/H^+ and Li^+/H^+ antiport. In plants this group is represented by proteins localizing at the chloroplast membrane (Ottow *et al.*, 2005; Barrero-Gil *et al.*, 2007)). McNhaD shows 76.8% protein sequence identity with AtNhaD1 of *A. thaliana.*

The second protein McSOS1 belongs to the phylogenetic cluster of SOS1 transporters (NhaP/SOS1 family of CPA1) and shows 61.4 % identity to AtSOS1 from *A. thaliana*, a well characterized transporter that catalyzes Na^+/H^+ exchange at the plasma membrane (Pardo *et al.*, 2006). The degree of identity is even higher when McSOS1 is compared with the transporter SjSOS1 from the halophyte plant *Suaeda japonica* (sequence identity of 74.1 %). The long C-terminus of McSOS1 also shows the cyclic-nucleotide binding domain typical for proteins of the NhaP/SOS1 family.

The three remaining cloned transporters belong to the IC- (Intra-Cellular) NHE/NHX subfamily of the CPA1 group. All plant NHX proteins characterized to date are members of the IC subfamily which also comprises animal and fungal antiporters (Pardo *et al.*, 2006). IC-NHE/NHX can be further split into two classes: Class I includes proteins that catalyze Na^+/H^+ or K^+/H^+ transport with equal affinity; Class II comprises antiporters that show a preference for K^+ over Na^+ as a substrate and that are found in membranes of the endosomal compartment of plants (Venema *et al.*, 2003). In *A. thaliana* members of class I (AtNHX1-4) are 56-87% similar to each other and localize to the vacuolar membrane. McNHX1 falls into this category and shows 74.6% and 76.6% similarity to AtNHX1 and AtNHX2, respectively. However, the highest similarity of McNHX1 can be found when compared to antiporters of halophyte plants: 92.2% with TtNHX1 from *Tetragonia tetragonioides* and 86.2% with AgNHX1 from *Atriplex gmelini*. The second cloned antiporter of the IC-NHE/NHX subfamily, McNHX2, belongs to the endosomal class II antiporters. AtNHX5-6 are members of this group; they are 79.0% similar to each other but exhibit only 21.0-23.0% similarity with class I isoforms (Pardo *et al.*, 2006). McNHX2 exhibits 71.0% and 75.7% similarity to AtNHX5 and AtHNX6, respectively. On the other hand, McNHX2 has less than 27.0% of sequence similarity with the other cloned NHX isoforms from *M. crystallinum*. Finally McNHX3 the fifth cloned antiporter of the IC-NHE/NHX subfamily, groups together with AtNHX3 and AtNHX4 (51.3% and 51.4% similarity, respectively). McNHX3 shows 57.5 % similarity to McNHX1.

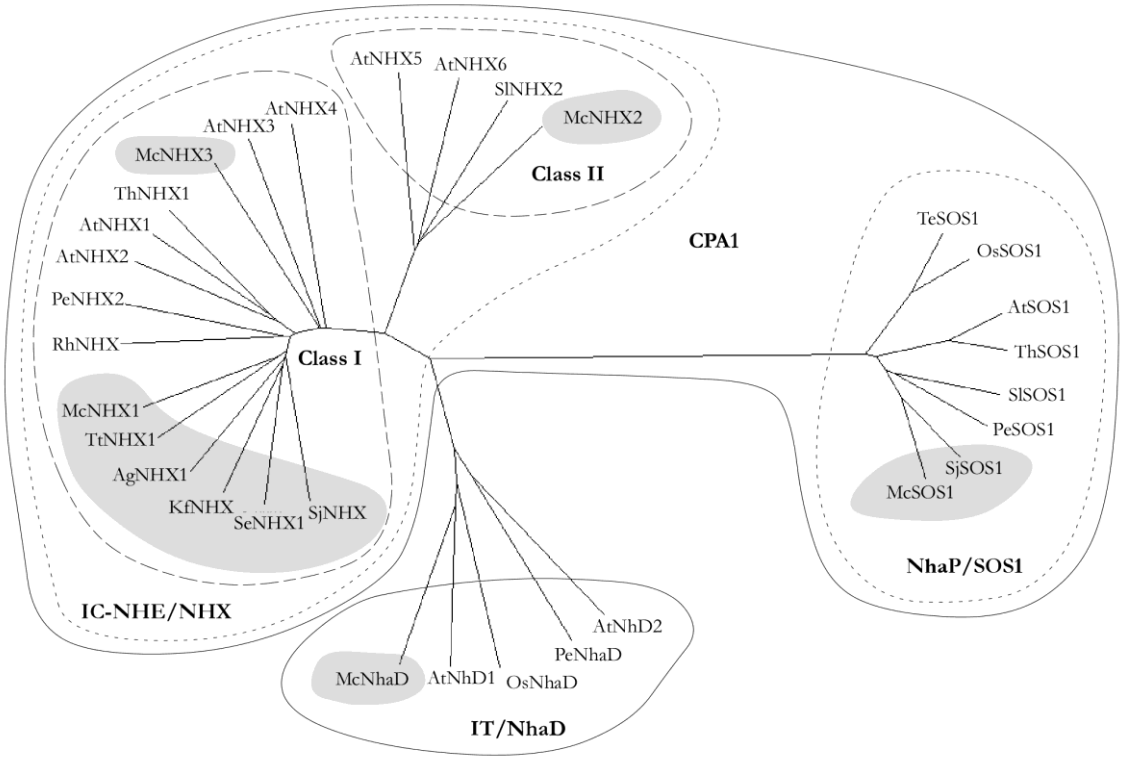

Figure 1. Phylogenetic tree of Na^+/H^+ antiporters. A multiple sequence alignment was generated using ClustalW and evolutionary distances were calculated by the neighbor joining method. The McNHX1, McNHX2, McNHX3, McSOS1 and McNhaD are from *Mesembryanthemum crystallinum*; AtNHX1, AtNHX2, AtNHX3, AtNHX4, AtNHX5, AtNHX6, AtSOS1, AtNhaD1 and AtNhaD2 are from *Arabidopsis thaliana*; RhNHX is from *Rosa hybrida*; PeNHX2, PeNhaD and PeSOS1 are from *Populus euphratica*; SjNHX and SjSOS1 are from *Suaeda japonica*; SlNHX2 and SlSOS1 are from *Solanum lycopersicum*; OsSOS1 and OsNhaD are from *Oryza sativa*; ThSOS1 and ThNHX1 are from *Thellungiella halophila*; TeSOS1 is from *Triticum aestivum*; KfNHX is from *Kalidium foliatum*; TtNHX1 is from *Tetragonia tetragonioides*; SeNHX1 is from *Salicornia europaea*; AgNHX1 is from *Atriplex gmelini*. Proteins of halophytes are labeled by a grey background.

The five Na^+/H^+ antiporters listed above comprise all of the putative members of these transporter families within the *M. crystallinum* EST repository at the NCBI data base. This however does not mean that there are no further proteins of this type because the database is not necessarily containing the entire genome. In order to search for remaining candidate sequences a pool of 50 representative sequences including all representative genes from all three families (NhaP/SOS1, IC-NHE/NHX and IT/NhaD) have been used to search the *M. crystallinum* repository. This procedure, however, gave no positive hits other than those already listed in Table 2. This already suggests that there are no further ESTs of the Na^+/H^+ type antiporter in the *M. crystallinum* database. This assumption is further supported by

experiments using RT-PCR on RNA extracted from leaves of untreated as well as NaCl treated plants. Degenerate primers were designed on a conserved region of the IC-NHE/NHX isoforms of the cloned Na^+/H^+ antiporters (forward 5'-GCVGGKTTTCARGTDAARAARAAGCA-3' and reverse 5'-ACWCCYTCHCCRAAHACHAGACTGTA-3'). This gene family was chosen because it comprises the highest number of isoforms and should thus provide the broadest probe for screening. The 20 amplicons sequenced all matched the genes already cloned. No further IC-NHE/NHX isoforms have been detected (data not shown).

In conclusion these data strongly indicate that all Na^+/H^+ antiporter expressed in leaves of *M. crystallinum* have indeed been cloned.

5.2 Prediction of transmembrane domains and cellular localization

In order to predict the number of transmembrane domains (TMD) of the cloned Na^+/H^+ antiporters a consensus prediction for transmembrane alpha helices was carried out using a list of 18 individual structural prediction programs (see Material and Methods, Table 1). The built-in consensus prediction was calculated by assigning a value of 1 to each amino acid predicted as part of a transmembrane alpha helices and a value of zero to the remaining amino acids. The average of the scores for each amino acid was ranged between 0 and 1 and determined the TMD consensus prediction. The results for each antiporter are plotted in Figure 2. Predictions of the widely-used program TMHMM v2 are reported for comparison (dotted lines in Fig. 2). An arbitrary threshold of 0.6 has been applied in order to include into a consensus TMD only amino acids which have positive scores in more than half of prediction tests. The results of this analysis are reported in Table 3.

According to Table 3 McNhaD contains 13 TMDs (10 TMDs calculated by TMHMM v2) and McSOS1 12 TMDs (10 by TMHMM v2). For McSOS1 11 programs out of 18 predicted that the fifth TMD is only 3 amino acids long (170-173). This would not allow to span the whole membrane and may suggest that it is not a real TMD. However, the number of predicted amino acids is strongly affected by the setting of the threshold of the respective programs used. For example, DAS-Tmfitter calculated an alpha-helix of three amino acids with the threshold of 0.6. Just lowering the threshold to 0.55 the consensus prediction gives a 17 amino acid long TMD. Moreover, the estimated consensus TMD prospect for McSOS1 is in agreement with the predicted structure of NhaP/SOS1-like exchangers, consisting of a N-terminal transmembrane region followed by a hydrophilic C-terminal extension that, in eukaryotic homologues, is remarkably longer than 600 residues (Pardo *et al.*, 2006).

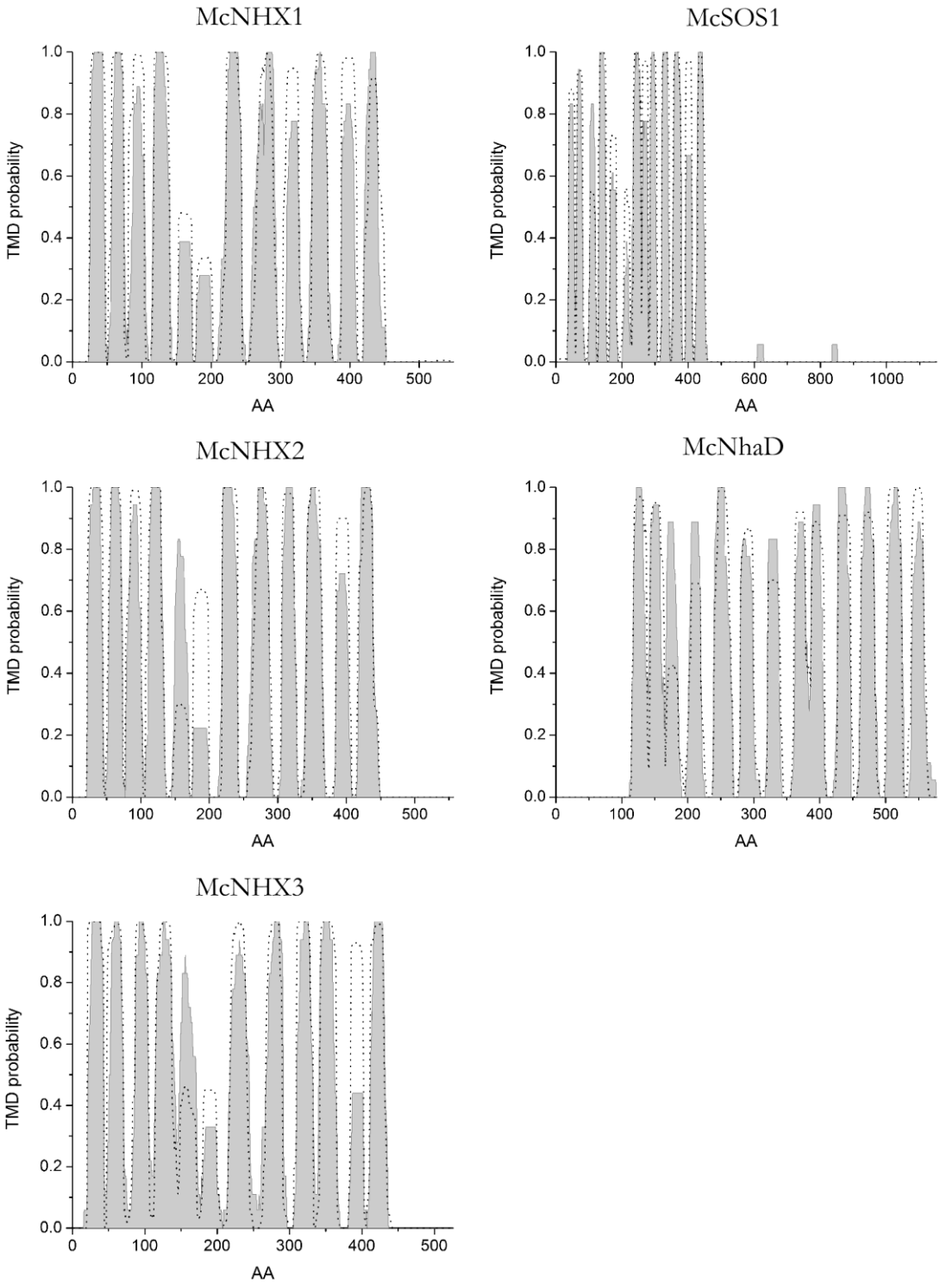

Figure 2. Predicted transmembrane domains (TMD) of the cloned Na^+/H^+ antiporters from *Mesembryanthemum crystallinum*. Data represent the average of 18 TMD prediction programs (see Materials and Methods). The prediction of TMHMM v2 is reported as reference (dotted lines). Cut off of 0.6 in the TMD probability was applied in order to define a certain region as transmembrane domain.

Table 3. Consensus of predicted TMDs for McNHX1, McNHX2, McNHX3, McNhaD and McSOS1 Na^+/H^+ antiporters of *Mesembryanthemum crystallinum.*

TMD	McNhaD	McSOS1	McNHX1	McNHX2	McNHX3
	577 aa	*1151 aa*	*549 aa*	*556 aa*	*526 aa*
1	118-135	39-53	26-45	23-42	23-43
2	142-158	63-78	57-74	54-72	53-70
3	168-182	103-118	88-103	82-99	87-104
4	204-219	132-150	117-138	112-131	116-139
5	240-261	170-173	222-244	150-164	149-166
6	280-298	234-257	266-291	219-240	219-242
7	321-337	262-278	311-325	263-287	271-291
8	363-378	285-302	345-367	306-324	311-330
9	387-404	321-338	388-406	342-364	341-361
10	427-445	356-380	423-440	386-401	413-431
11	463-483	394-410		419-438	
12	503-524	427-445			
13	541-557				

For the antiporter belonging to the IC-NHE/NHX family 10 TMDs were predicted for McNHX1, 11 TMD for McNHX2 and 10 TMD for McNHX3. The TMHMM v2 algorithm for comparison suggests 11, 10 and 10 TMDs for the respective proteins.

In a subsequent analysis a putative consensus prediction of the cellular localization of the antiporters has been performed. Twelve individual programs which screen the protein for targeting sequences have been considered (see Material and Methods, Table 1). The analysis discriminates between chloroplast (C), mitochondrion (M), inner compartments or secretory pathway (I) and other locations (O); these results are summarized in Table 4.

According to the predictions McNhaD is most likely localized in the plastidial membrane. McNHX1 is predicted to be sited at membranes of inner compartments or the secretory pathway. This is in agreement with a tonoplast localization of other known vacuolar antiporters which are similar to McNHX1 (see Fig. 1) (Kagami and Suzuki, 2005; Hamada *et al.*, 2001; Apse *et al.*, 1999).

Table 4. Prediction of the subcellular localization of McNHX1-3, McNhaD and McSOS1 proteins; C for chloroplast, M for mitochondrion, I for inner compartments or secretory pathway, O for other locations, TP for the number of amino acids forming the transit peptide. Best predictions are marked with thick line. Localizations which are included in the prediction program are labeled grey. Localizations which are not included in the prediction program are marked by (–)

		ChloroP v1.1	iPSORT	MITOPRED	MitoProt II v1.0a4	PCLR v0.9	PProwler v1.1	PrediSi	Predotar	PredSL	SignalP v3.0_HMM	SignalP v3.0_NN	targetP v1.1
McNHX1	**C**	0.48		-	-	0.03	0.02	-	0.02	0.00	-	-	0.03
	M	-			0.02	-	0.01	-	0.01	0.00	-	-	0.04
	S	-		-	-	-	**0.79**	0.47	0.02	**1.00**	0.05		**0.52**
	O	-	-	-	-	-	0.17	-	**0.96**	-	-	-	0.40
	TP	25	-	-	-	-	-	44	-	44	41	41	41
McNHX2	**C**	0.44		-		0.02	0.03	-	0.00	0.00	-	-	0.15
	M	-			0.08	-	0.04	-	0.01	0.03	-	-	0.17
	S	-		-	-	-	0.06	0.40	0.00	**0.99**		0.01	0.03
	O	-	-	-	-	-	**0.87**	-	0.99	-	-	-	**0.85**
	TP	23	-	-	-		-	40	-	40	40	40	-
McNHX3	**C**	0.49		-		0.10	0.43	-	0.13	0.00	-	-	0.34
	M	-			0.04	-	0.04	-	0.01	0.00	-	-	0.11
	S	-		-	-	-	0.23	0.48	0.01	**1.00**		0.00	0.03
	O	-	-	-	-	-	0.30	-	**0.86**	-	-	-	**0.69**
	TP	8	-	-	-			44	-	44	44	44	-
McNhaD	**C**	**0.57**		-	-	**1.00**	**0.98**	-	**0.78**	**1.00**	-	-	**0.91**
	M	-		**0.80**	**0.99**	-	0.01	-	0.06	0.00	-	-	0.35
	S	-		-	-	-	0.00	0.04	0.00	0.00	0.01		0.01
	O	-	-	-	-	-	0.00	-	0.20	-	-	-	0.01
	TP	35	-	-	64	-	-	17	-	68	17	-	35
McSOS1	**C**	0.45		-	-	0.02	0.02	-	0.01	0.00	-	-	0.06
	M	-			0.23	-	0.05	-	0.01	0.00	-	-	0.02
	S	-		-	-	-	0.34	0.40	0.04	**0.77**	0.04		**0.57**
	O	-	-	-	-	-	**0.59**	-	**0.95**	-	-	-	0.47
	TP	23	-	-	-	-	-	54	-	54	30	-	19

McNHX2 and McNHX3 are predicted to be localized in inner or in other compartments (Table 4). From the consensus prediction the putative localization of McSOS1 is not clear. Considering that the highly homologous antiporter AtSOS1 has been demonstrated to localize at the plasma membrane (Qiu *et al.*, 2002) the predicted localization of McSOS1 can also be interpreted as plasma membrane localization. Taken together the analysis suggests that all the cloned antiporters are transmembrane proteins; the *in silico* prediction of their

cellular localization is in agreement with the localization of other phylogenetic related proteins.

5.3 Functional complementation of *Saccharomyces cerevisiae* mutant strains

It should be stated that the above reported *in silico* analysis of protein structure and localization are only a prediction for the real structure and function of a protein. However, the experimental results confirm that the cloned transporters have TMDs and localize at cellular membranes.

Thus, in order to investigate the function of proteins encoded by the cloned antiporter genes, functional complementation tests of *Saccharomyces cerevisiae* mutant strains have been performed. Genes encoding for McSOS1 and McNhaD have been inserted into the pYES2 expression plasmid and expressed in the yeast mutant e*na1-4 nhx1 nha1* (AB11c, gently provided by Adam Bertl, Technische Universität Darmstadt). This yeast mutant is highly Na^+ sensitive so that the expression of an active Na/H^+ antiporter should support survival of these cells under Na^+ stress. Yeast cells were grown on SD–Ura Gal/Raf medium supplemented with 200 mM NaCl. In contrast to the yeast wild strain (W303) the yeast mutant showed nearly no growth at high NaCl concentration (Fig. 3A). This defect could partly be complemented by expression of McSOS1 and McNhaD in the mutant strain (Fig. 3A). The results of these experiments therefore suggest that both antiporters catalyze Na^+ efflux at the plasma membrane. To confirm these results Na^+ accumulation was analyzed in wt yeast, mutant strains and in the yeast mutants expressing the cloned antiporter McSOS1 and McNhaD. Cells grown in liquid medium supplemented with 200 mM NaCl were harvested at saturation of growth and the cellular Na^+ content was determined. In Figure 3B results are presented as the ratio of the Na^+ content measured in the mutant strain or mutant cells expressing McSOS1 or McNhaD over the Na^+ content of the control strain (W303). The results show that Na^+ accumulation is highest in the mutant strain which accumulated 2.8 times more Na^+ than the control strain (Fig. 3B). In mutant cells expressing McSOS1 or McNhaD Na^+ accumulation was significantly lower (Fig. 3B). In these cells the Na^+ content was only 2.3 times the amount found in the control strain. The significance of the differences was statistically verified by the t-student's test. The probability P that Na^+ accumulation of the wt and the mutants is similar is lower than 0.1. In conclusion these results demonstrate that the antiporter McSOS1 or McNhaD are functional proteins. They can partially complement the Na^+ efflux defect of *S. cerevisiae* mutant strains and both

localize at the plasma membrane in yeast as was previously shown for AtSOS1 (Quintero *et al.*, 2002). Therefore the cloned antiporter genes most likely encode for functional Na^+/H^+ antiporters.

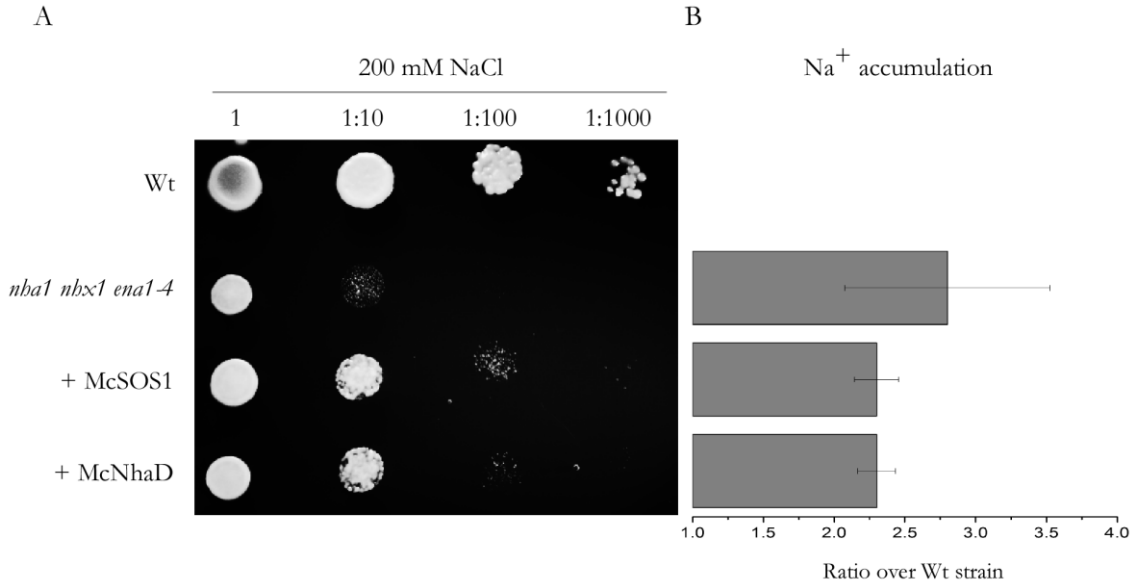

Figure 3. Functional complementation of the salt sensitive mutant *nha1 nhx1 ena1-4* (AB11c) of *Saccharomyces cerevisiae* by McSOS1 and McNhaD. pYES2 empty vector was introduced into the W303 wt and AB11c mutant. The same vector carrying the full-length genes for McSOS1 or McNhaD was expressed in AB11c mutant. (**A**) Ten-fold serial dilutions were spotted onto SD-Ura Gal/Raf supplemented with 200 mM NaCl and plates were incubated at 30° C for 2 days. (**B**) Ratio of Na^+ contents measured in respective yeast cells over the Na^+ content of the control strain (W303). Yeast cells were grown in SD-Ura Gal/Raf liquid medium supplemented with 200 mM NaCl and washed three times with distilled water before Na^+ determination. Error bars (n=3) ± SD

To investigate the function of cloned isoforms of the IC-NHE/NHX subfamily the *nhx1* mutant strain of *S. cerevisiae* (YDR456W, Euroscarf) was used and the Hygromycin B sensitivity of cell growth was analyzed. Hygromycin B is a toxic cation that accumulates in cells upon an electrochemical proton gradient (Darley *et al.*, 2000). The yeast ScNHX1 vacuolar antiporter has been found to be not only involved in Na^+ transport but also to play an important role in the compartmentation of Hygromycin B into the vacuoles (Fukuda *et al.*, 2004; Gaxiola *et al.*, 1999; Kagami and Suzuki, 2005). Transport of Hygromycin B instead of Na^+ can thus be used as a marker transport process to determine if the cloned McNHXs isoforms exhibit a vacuolar function in yeast. Yeast cells were grown on a medium supplemented with 100 μg/ml Hygromycin B. Under these conditions only the mutant strain expressing McNHX1 was found to grow similar to the control strain (B4741) (Fig. 5A). Mutants expressing McNHX2 and McNHX3 isoforms were not able to complement

Hygromycin B dependent inhibition of growth (Fig. 4A). This suggests that only McNHX1 functions as an antiporter at the vacuolar membrane of yeast.

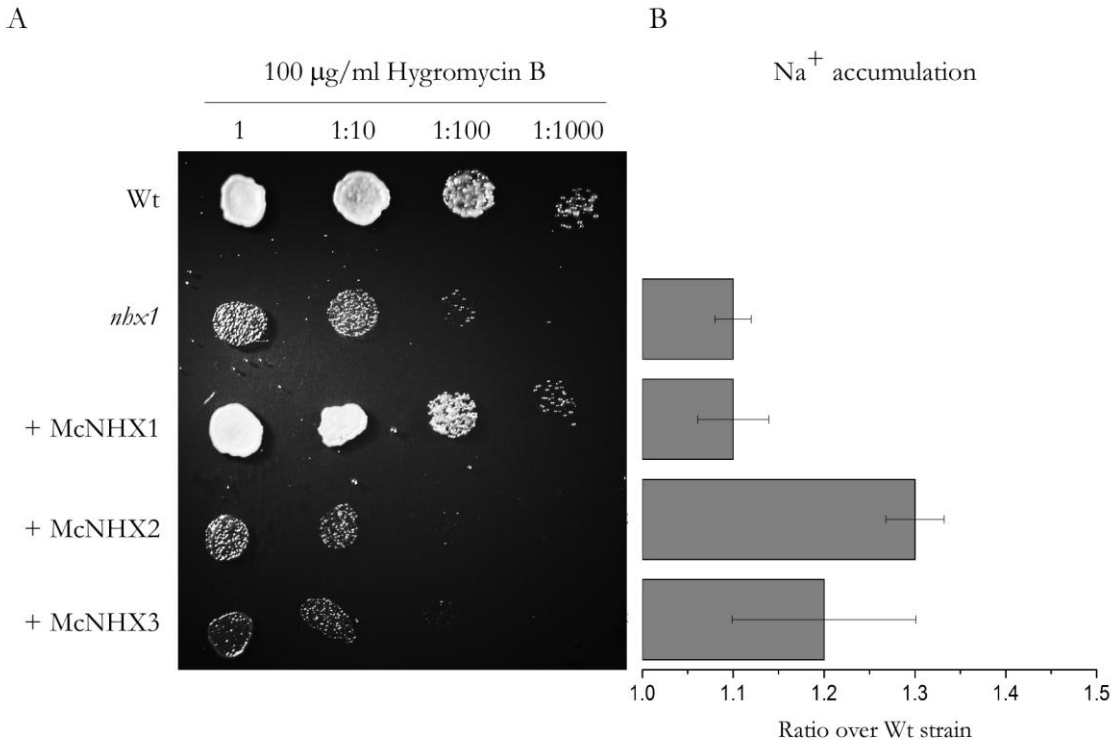

Figure 4. Functional complementation of the Hygromycin B sensitive mutant *nhx1* (YDR456W) of *Saccharomyces cerevisiae* by McNHX1, McNHX2 and McNHX3. pYES2 empty vector was introduced into the B4741 wt and the YDR456W mutant. The same vector carrying the full-length genes for McNHX1, McNHX2 or McNHX3, was expressed into the YDR456W mutant. (**A**) Ten-fold serial dilutions were spotted onto SD-Ura Gal/Raf supplemented with 100 µg/ml Hygromycin B and plates were incubated at 30°C for 2 days. (**B**) Na^+ content of respective yeast cells. Cells were grown in SD-Ura Gal/Raf liquid medium supplemented with 500 mM NaCl. Cells were washed three times with distilled water before Na^+ determination. Data are ratios of the Na^+ content measured in the respective yeast cells over the control strain (BY4741). Error bars (n=3) ± SD

To further analyze the function of the three McNHX isoforms the accumulation of Na^+ was determined. Cells were grown in liquid medium supplemented with 500 mM NaCl harvested at saturation of growth and the cellular Na^+ content was measured. Data are presented as ratios of the Na^+ content measured in respective yeast cells over the Na^+ content of the control strain (B4741). The results shown in Fig. 4B do not reveal any difference in Na^+ accumulation between the yeast mutant *nhx1* and the mutant expressing McNHX1. In both cases the Na^+ content was not significantly higher than in control cells. However, when McNHX2 and McNHX3 were expressed in the mutant strain the internal Na^+ content

increased significantly up to 1.3 and 1.2 times, respectively, compared to the control. The significance of the differences was verified by t-student's test ($P<0.05$)

These results show that by complementing the Hygromycin B sensitivity of yeast *nhx1* mutants (YDR456W), McNHX1 but not McNHX2 and McNHX3 can function as ScNHX1 does at the *S. cerevisiae* vacuolar membrane. Interestingly these complementation studies also suggest that the mechanism of Hygromycin B sensitivity and vacuolar Na^+ accumulation in yeast are not identical. When McNHX2 and McNHX3 are expressed yeast *nhx1* cells accumulate a higher amount of Na^+ compared to McNHX1. This was not expected with respect to Hygromycin B sensitivity and thus it is apparently in contrast to complementation tests. However, the yeast *nhx1* mutant is not as sensitive to Na^+ as the e*na1-4 nhx1 nha1* (AB11c). In a medium supplemented with Na^+ 500 mM YDR456W accumulates 689±131 nmol $Na^+/10^8$ cells, which is very similar to the control B4741 that is able to store up to 575.3±147 nmol $Na^+/10^8$ cells. Hence the Na^+ efflux in the *nhx1* mutant is apparently efficient enough to assure a cytoplasmic Na^+ level similar to the control. Since the cytoplasmic Na^+ concentration is not changing at all in the *nhx1* mutant, McNHX1 when expressed at the vacuolar membrane of that mutant may not be enough competitive for a high Na^+ accumulation into the vacuole. Consequently the cellular Na^+ content does not change in respect to the control strain. In contrast McNHX2 and McNHX3 in the case they are expressed in endomembranes may mediate the Na^+ influx by endocytic vesicles accumulating Na^+ directly from the external medium. In that case an increase in the cellular Na^+ content is expected and has been detected.

5.4 Functional complementation of McNhaD in *Escherichia coli*

The data of the phylogenetic analysis and the *in silico* prediction of cellular localization imply that McNhaD is operating as a chloroplast Na^+/H^+ antiporter. However, functional complementation studies of McNhaD in yeast suggest that it is localized at the plasma membrane (see Chapter 3.3). These apparently contradicting results can be explained by the fact that yeast does not contain chloroplasts. Proteins containing plastidial targeting signals (as does McNhaD) have previously been shown to be targeted to the plasma membrane when expressed in yeast (Duy *et al.*, 2007). Chloroplasts are evolutionary more similar closed to prokaryotes than to yeast. In order to investigate the function of McNhaD as a plastidial Na^+/H^+ antiporter, functional complementation tests for McNhaD have been performed with the *nhaA nhaB* mutant of *E. coli* (EP432, gently provided by Thomas Teichmann, University of Giessen), the only available prokaryote defective in Na^+/H^+ antiport. This *E.*

coli mutant is defective in the two main bacterial Na^+/H^+ antiporters, *nhaA* and *nhaB*. For the complementation assay McNhaD has been inserted into the inducible expression vector pQE60 and expressed in EP432 salt sensitive cells. Beside Na^+ sensitivity also the sensitivity to Li^+ was tested since the EP432 mutant may spontaneously convert into the MH1 mutants. This mutant is Na^+ resistant but it is still Li^+ sensitive. Lithium is toxic at approximately one-tenth of the concentration of Na^+; also Li^+ appears to share some signaling and transport pathways with Na^+ causing symptoms similar to salt stress (Harel-Bronstein et al., 1995).

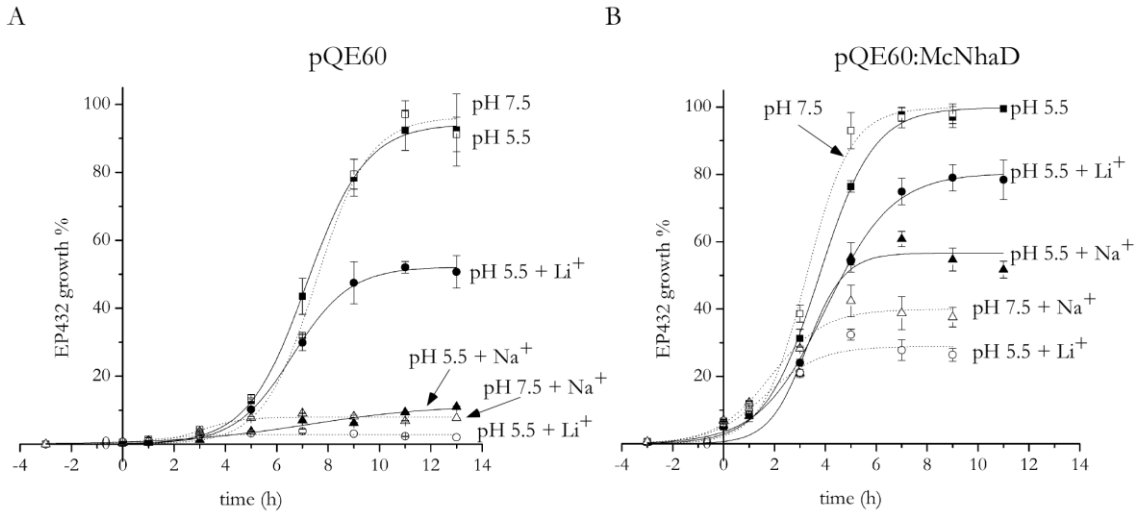

Figure 5. Effects of pH on *E. coli* EP432 functional complementation with McNhaD. EP432 *nhaA nhaB* mutant was grown on LBK plates at pH 5.5 (closed signs) or 7.5 (open signs), supplemented with 5 mM LiCl (● and ○) or 200 mM NaCl (▲ and △). (**A**) pQE60 empty plasmid; (**B**) pQE60 carrying the McNhaD gene from codon 36 to 577. Error bars (n=3) ± SD; data are presented as percentage of the maximum growth level reached at each tested pH.

Control strains carrying the pQE60 empty vector showed similar growth kinetics at both pH conditions applied, with a $t_{1/2}$ of 7.2 h at pH 5.5 and 7.6 h at pH 7.5 (Fig. 5 and Table 5). In contrast when 5 mM LiCl was added, a different growth characteristic was observed which was also depending on the pH of the medium. At pH 5.5 the growth was inhibited by 50% with respect to the untreated condition; at pH 7.5 the growth was nearly abolished. Moreover in presence of 200 mM NaCl the growth did not exceed the 10% of the growth found under control conditions at pH 5.5 as well as at pH 7.5 (Fig. 5A).

Table 5. Growth percentage of EP432 *E. coli* mutant cells carrying an empty plasmid or expressing the McNhaD gene under media supplemented with 5 mM LiCl or 200 mM NaCl. Non-linear curve fitting was applied using the equation [2]; R^2 is for Pearson's correlation coefficient; n.t. is for not-treated cells

pH	Treatment	Strain	% growth	R^2
5.5	n.t.	+ McNhaD	99.5	0.99
	+ LiCl	EP432	55.1±1.6	0.99
		+ McNhaD	80.0±4.1	0.99
	+ NaCl	EP432	13.8±0.6	0.96
		+ McNhaD	55.9±3.7	0.98
7.5	n.t.	+ McNhaD	98.4	0.99
	+ LiCl	EP432	2.9±0.1	0.83
		+ McNhaD	28.9±1.0	0.96
	+ NaCl	EP432	7.9±0.3	0.97
		+ McNhaD	39.9±3.1	0.98

However, the growth rate of LiCl treated EP432 cells expressing the McNhaD protein nearly reached that of the untreated control (Fig. 5B). At pH 5.5 the growth of cells treated with LiCl and carrying the pQE60:McNhaD plasmid reaches up to 80% of the untreated control; at pH 7.5 the mutants reach about 30% of the control. When the McNhaD expressing cells were treated with NaCl the recovery of the growth rate was more consistent. Here the growth reached almost 56% and 40% of the growth measured under control conditions at pH 5.5 and pH 7.5, respectively. In Figure 6 the percentage of growth recovery of *E. coli* mutant and complemented cells with respect of the untreated control is reported.

In the presence of LiCl cell growth reached 55% of the untreated condition at pH 5.5. When McNhaD was expressed this ratio increased up to 80%. Similar results were obtained with cells grown at pH 7.5, moving from 3% up to nearly 29% of the untreated control growth. The effect of recovery from inhibition was stronger in the presence of 200 mM NaCl (Figure 6B). Here, the EP432 growth increased from 14% and 8% up to 56% and 40% of the control sample, at pH 5.5 and 7.5 respectively. In summary McNhaD partially complements the negative effect of LiCl and NaCl on the EP432 mutation in *E. coli*. This McNhaD mediated recovery from inhibition is a function of pH. Together the results demonstrate that McNhaD functions as a Na^+/H^+ antiporter.

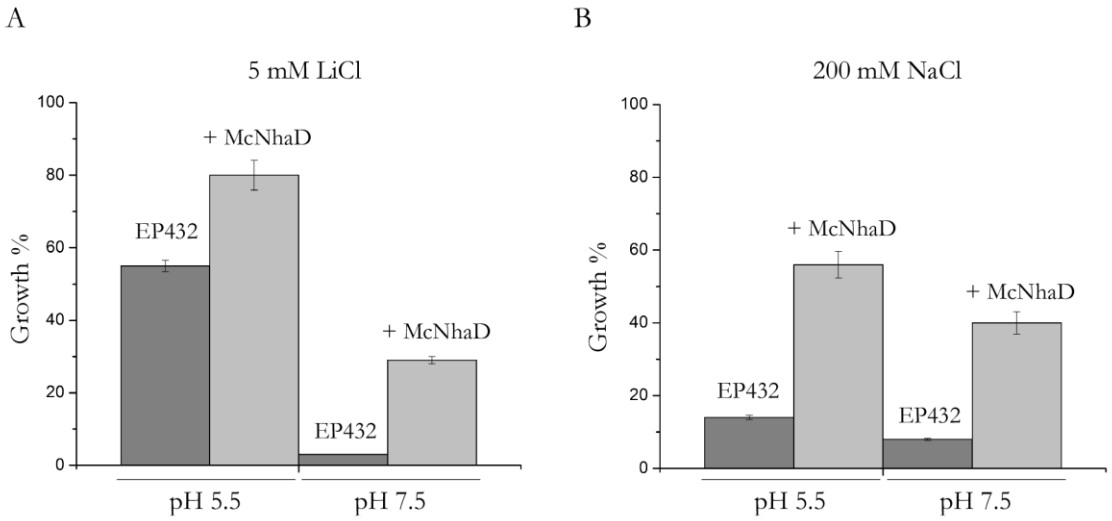

Figure 6. Recovery rates of McNhaD functional complementation in EP432 *E. coli* mutant. EP432 cells were treated with 5 mM LiCl (**A**) or 200 mM NaCl (**B**). Bacteria were grown in LBK medium supplemented with 5 mM LiCl or 200 mM NaCl at pH 5.5 and 7.5. Growth are expressed as percent over the maximum growth of untreated EP432 mutants, transformed with empty vector (EP432) or pQE60:McNhaD (+McNhaD). Error bars (n=3) ± SD; differences are significant according to student's t-test ($P < 0.05$).

5.5 Salt induced expression of Na^+/H^+ antiporters in *Mesembryanthemum crystallinum*

The results of functional complementation assays with yeasts suggest a key role for some of the cloned antiporters in the vacuolar Na^+ compartmentation. In order to determine the importance of the cloned Na^+/H^+ antiporters in plants under salt stress the transcript levels were analysed by real-time PCR in both, leaves and roots in response to NaCl treatment of plants. Results from these experiments are summarized in Figure 7. Data represent the average of three independent analyses. The housekeeping gene actin was chosen as reference gene because its expression was less affected by NaCl treatment than the expression of tubulin and 18S rRNA. Transcript levels of the transporters under investigation were related to the actin transcript level at the respective time point and normalized to the gene expression level of the transporter at day zero of NaCl treatment (metabolic state of plants: C3 photosynthesis).

The analysis reveals that the expression of McNhaD, McSOS1 and McNHX1 was induced in leaves but not in roots by NaCl treatment (Fig. 7).

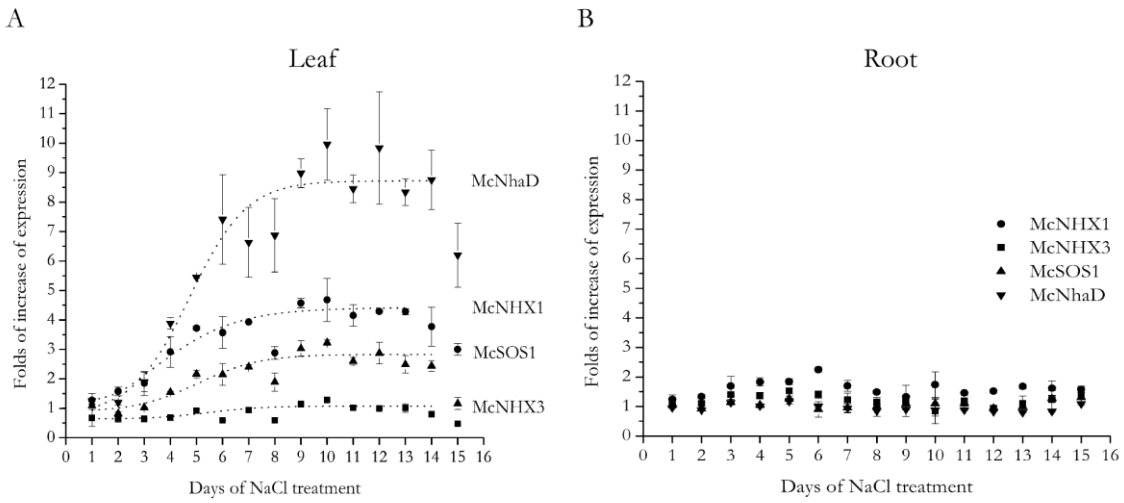

Figure 7. Time course of transcript levels of the putative Na^+/H^+ antiporters McNHX1 (●), McNHX3 (■), McSOS1 (▲) and McNhaD (▼) in leaf (**A**) and root cells (**B**) of *Mesembryanthemum. crystallinum* upon salt treatment. Transcript levels were determined by real-time PCR. Values were calculated as ratios of the actin amplification level. Samples analysed are mixed samples of three plants harvested at the same time point. Data represent mean values (n=3) ± SD. Data are fitted by a logistic curve [2]

In roots only a slight increase of McNHX1 transcripts between day 3 and day 6 of stress induction was observed. In shoots the majority of the transporters are up-regulated in response to salt stress. Here only the transcript level of McNHX3 did not change (Fig. 7A). Transcripts of McNHX2 were neither detected in leaves nor in roots in real-time PCR experiments indicating an expression level of this isoform below the detection limit of the analysis. Expression levels of McNhaD, McSOS1 and McNHX1 started to increase in leaves after day 3 of NaCl treatment. After about 8 days the increase in expression saturated. Interestingly the expression levels of transcripts of all three genes started again to decrease at day 14 to day 15 of NaCl stress.

To compare the expression data in a quantitative manner the data points of McNhaD, McSOS1 and McNHX1 expression were fitted by the logistic function (see Materials and Methods, equation 2). The fitting parameters are listed in Table 6 and the resulting curves are shown as dotted lines in Figure 9. Data points beyond 14 days of stress, e.g. the late decrease in expression, were not included in the fitting.

According to parameters of fits (Table 6), the transcript level of McNhaD exhibited the strongest response to NaCl treatment; it increases 7.8±0.42 times with respect to the level at day zero of stress application.

Table 6. Summary of the characteristic parameters of the fitting curves for Na^+/H^+ antiporters expression in leaf. R^2: Pearson's correlation coefficient; A_{max}: saturation level according to equation [2]; $t_{1/2}$: halftime of the saturation level

Tissue	Gene	Ratio of increase with respect to C3 state	$t_{1/2}$ (days)	R^2
Leaf	McNHX1	3.6±0.5	4.0±0.1	0.97
	McSOS1	1.8±0.1	5.0±0.4	0.94
	McNhaD	7.8±0.4	4.7±0.1	0.98

The response of McNHX1 was also pronounced with an increase of transcript level of 3.6±0.5 times. McSOS1 showed the smallest increase in transcription level; it increased only 1.8±0.1 times. With regards to the time required to approach half maximum expression ($t_{1/2}$), McNHX1 showed the fastest response ($t_{1/2}$ of 4.0±0.1 days) followed by the expression of McNhaD ($t_{1/2}$ of 4.7±0.1 days). The gene with the slowest response time was McSOS1 with a $t_{1/2}$ of 5.0±0.4 days. The comparison of the $t_{1/2}$ values reveals that the burst of the expression of Na^+/H^+ antiporters in leaves occurred for all proteins within a small time window of around day 4 to day 5 of NaCl treatment. In contrast the amplitude of gene expression was gene specific and ranged between an approximately 2 and 8 fold increase.

In conclusion, the expression studies indicate that under high salinity transcript levels of McNhaD, McSOS1 and McNHX1 antiporters increased in leaves but not in roots in a gene specific manner supporting their key role in intracellular Na^+ compartmentation of *M. crystallinum*.

5.6 Localization of McNhaD after heterologous expression in *Vicia faba* guard cells

Experimental evidences support the plasma membrane and internal membrane localization of members of the NhaP/SOS1 and IC-NHE/NHX families of exchangers (Apse *et al.*, 2007; Pardo *et al.*, 2006; Shi *et al.*, 2000). In contrast little is known about cellular localization of the IT/NhaD family members. Up to date only localization studies of PpNhaD1 from the moss *Physcomitrella patens* have been performed (Barrero-Gil *et al.*, 2007). However, there are no data available from *Spermatophyta*. For this reason McNhaD was fused to GFP (McNhaD:GFP) and its subcellular localization investigated by expressing the protein transiently in *Vicia faba* leaves. The *V. faba* was used as a heterologous expression system

because for *M. crystallinum* no methods for heterologous expression of proteins are established.

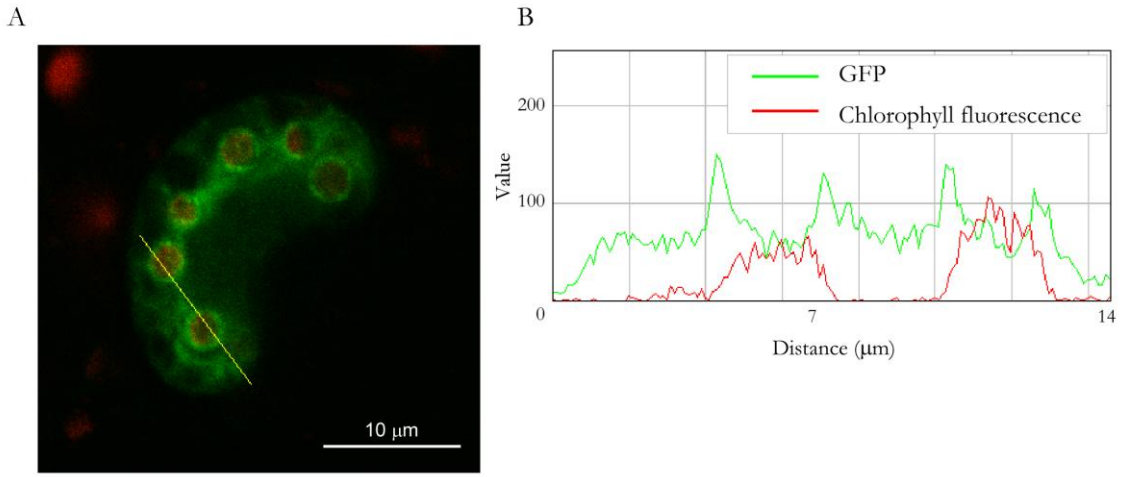

Figure 8. Localization of McNhaD:GFP in *Vicia faba* guard cells. (**A**) Cross section of a guard cells showing McNhaD:GFP (green) expression at membrane of chloroplasts (red) and to a lesser extent at other endomembranes compartments and in the cytosol; scale bar: 10 µm (**B**) Intensity plot along the line shown in A of GFP (green) and chlorophyll auto-fluorescence (red).

In Figure 8A the localization of McNhaD:GFP in *V. faba* cells is reported. It is evident from comparison with the chlorophyll auto-fluorescence (red) that McNhaD is found mainly around the chloroplasts suggesting that it is located in the membrane system of chloroplast in stomata cells of *V. faba*. This is supported by the intensity profile of GFP and chlorophyll auto-fluorescence shown in Figure 8B. These data indicate that McNhaD is surrounding the chlorophyll fluorescence. Hence, the protein is probably localized in the inner or outer chloroplast membrane. The resolution of this optical detection is not high enough to discriminate in which of the plastidial membranes McNhaD localizes.

Taken together the data support a localization of the protein in the plastids. This experimentally determined localization is in good agreement with the aforementioned *in silico* localization analysis. Therefore these data indicate that McNhaD is a Na^+/H^+ exchanger of the chloroplast membrane. Together with the higher level of expression upon NaCl treatments, these data strongly suggest an involvement of chloroplasts in the Na^+ accumulation mechanisms of the halophyte *M. crystallinum*.

5.7 Accumulation of Na^+ in chloroplasts under salt stress

Several of the experimental data described above suggest that McNhaD is playing an important role in NaCl accumulation in chloroplasts of *M. crystallinum* upon NaCl stress. In order to confirm this role, Na^+ content of chloroplasts has been determined over a period of several days after stressing pants with NaCl.

When leaf cross sections of *M. crystallinum* were stained with the Na^+-sensitive dye CoroNa green a strong fluorescent signal was always detected in internal organelles of mesophyll cells (Fig. 9A). A more detailed analysis revealed that the Na^+ signal co-localized with the chlorophyll auto-fluorescence (Fig. 9B). This suggests that the maximum of the Na^+ signal originates from chloroplasts. Apparently chloroplasts of *M. crystallinum* accumulated considerable amounts of Na^+ when subjected to high salinity. However, CoroNa green is not a ratiometric dye. Hence, it does not allow a quantitative estimation of the plastidial Na^+ content from fluorescence intensity measurements.

For a more quantitative assessment chloroplasts were isolated from plants at different time points after NaCl treatment and the plastidial Na^+ content was determined. Calculation of Na^+ concentrations was carried out by using osmotically active volumes for intact chloroplasts of *M. crystallinum* of either 20 µl/mg or 30 µl/mg. These chloroplast volumes were previously determined by Demming *et al.* (1983 and 1986) for *M. crystallinum* plants either in the state of C3 photosynthesis (20 µl/mg chlorophyll) or for plants performing CAM induced by NaCl stress (30 µl/mg chlorophyll).

Data points from the time course of Na^+ accumulation in chloroplasts were fitted with both chloroplast volumes by a logistic function (see Materials and Methods, equation 2). Accumulation of Na^+ in the plastidial compartment occurred fast and reached half maximal concentration with a $t_{1/2}$ of 4.1±0.1 days after NaCl treatment. Fitting the data ($R^2 = 0.97$) revealed a maximum Na^+ accumulation in the range of 85.0±8.8 to 127.4±13.2 mM, depending on the osmotic volume considered for calculation. These data confirm that chloroplasts accumulate Na^+ ions in *M. crystallinum* mesophyll cells upon NaCl treatment. The Na^+ content increases in response to the salt stress by a factor of 9.7. This accumulation is likely mediated by the chloroplast Na^+/H^+ antiporter, McNhaD, whose transcript level increases under NaCl stress. The plastidial Na^+ accumulation process occurs early around day 4 of NaCl treatment and it achieves a maximal Na^+ accumulation over a period of only two days.

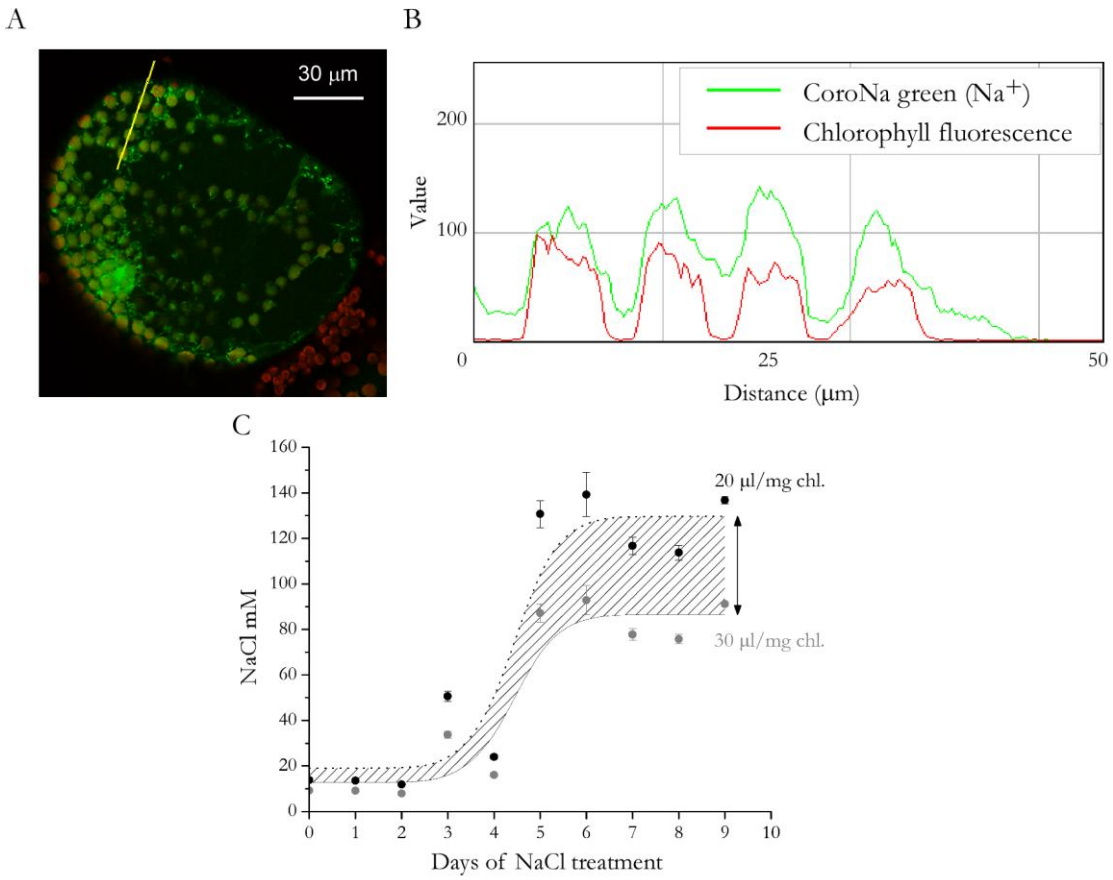

Figure 9. Na^+ accumulation in chloroplasts of *Mesembryanthemum crystallinum*. (**A**) Cross section of a mesophyll cells after 12 days of NaCl treatment; cells were stained with CoroNa green (E_x 488 nm, E_m 505-540 nm; green) red corresponds to chlorophyll fluorescence (E_x 488 nm, E_m 600-700 nm; red); scale bar: 30 µm; (**B**) intensity plot along the line shown in A of CoroNa green (green) and chlorophyll auto-fluorescence (red); (**C**) time curse of Na^+ accumulation in chloroplasts during plant NaCl treatment by assuming 20 µl/mg chlorophyll (▼) or 30 µl/mg chlorophyll (▲), as reported in Demming *et al.* (1983). Sparse line area represents the calculated range of concentrations for Na^+ accumulation in chloroplasts. Error bars (n=3) ± SD; data are fitted with a logistic equation [2]

5.8 Physiological parameters of *Mesembryanthemum crystallinum* L. upon salt treatment

In order to investigate the correlation between the expression characteristics of Na^+/H^+ antiporters and Na^+ accumulation in *M. crystallinum* plants some basic physiological parameters related to the adaptation of plants to high salinity and CAM induction have been monitored. To allow a direct correlation of data identical plant material has been used for the expression studies of Na^+/H^+ antiporters and the determination of the physiological parameters described below.

Plants of *M. crystallinum* were watered with 400 mM NaCl in tap water for up to 15 days. Leaf and root tissue of three individual plants were harvested at indicated time points. The material was pooled and subjected to analyses. The physiological parameters determined were: the concentration of Na^+, K^+, Mg^{++}, Ca^{++}, the Na^+/K^+ ratio, the concentration of malic acid, leaf osmolarity and proline concentration. Data from the multi-parameter analysis are summarized in Figure 9. Data points of individual measurements were fitted by a logistic function (see Materials and Methods, equation 2; dotted lines in Figure 10). The parameters from the curve fittings are presented in Table 7.

In leaf tissue the content of Na^+ as well as K^+ increased significantly upon NaCl treatment (Fig. 10A and Table 7). The leaf Na^+ content increased slowly ($t_{1/2}$ 11.7±1.5 days) and reached an estimated concentration of 0.85±0.12 μmol/g FW at saturation over the 15 days of NaCl stress. The increase in K^+ content in leaf cells occurred considerably faster ($t_{1/2}$=3.8±0.1 d) and reached a final level of 0.15±0.01 μmol/g FW within 15 days of NaCl treatment. In root tissue accumulation of K^+ and Na^+ occurred with similar kinetics as in leaves (Fig. 10B and Table 7) and both ions reached equal maximum content at the estimated saturation level: 0.25±0.01 μmol/g FW. However, the final concentration of Na^+ was much (3.4 times) lower in roots than in leaves while K^+ was on average 1.7 times higher in roots than in leaves.

The Na^+/K^+ ratio is an important parameter to follow net accumulation of Na^+ in plant cells. It is strictly regulated in order to keep the cytoplasmic Na^+ concentration low with the goal to prevent the interference of toxic Na^+ with metabolic processes. The Na^+/K^+ ratio of leaves increased noticeably starting at day 3 to day 4 after the onset of NaCl treatment. This increase reflects the accumulation of considerable amounts of Na^+ in leaf cells (see Fig. 10A). In contrast the Na^+/K^+ ratio of roots did not respond to NaCl treatment throughout the experiment.

In summary these data show a 3.4 times higher Na^+ accumulation in leaves compared to root tissue (Table 7). Na^+ is however also accumulated in roots but due to a higher compensative accumulation of K^+ the Na^+/K^+ remains unchanged.

Divalent cations Mg^{++} and Ca^{++} did not show any significant response to NaCl treatment neither in leaves nor in roots.

Malate accumulation was monitored as a marker for CAM induction in *M. crystallinum* (Winter and Willert, 1972) (Figure 10D). The malate concentration of leaf cell sap increased markedly after day 5 into NaCl treatment with a $t_{1/2}$ at 8.4±0.1 days (Table 6).

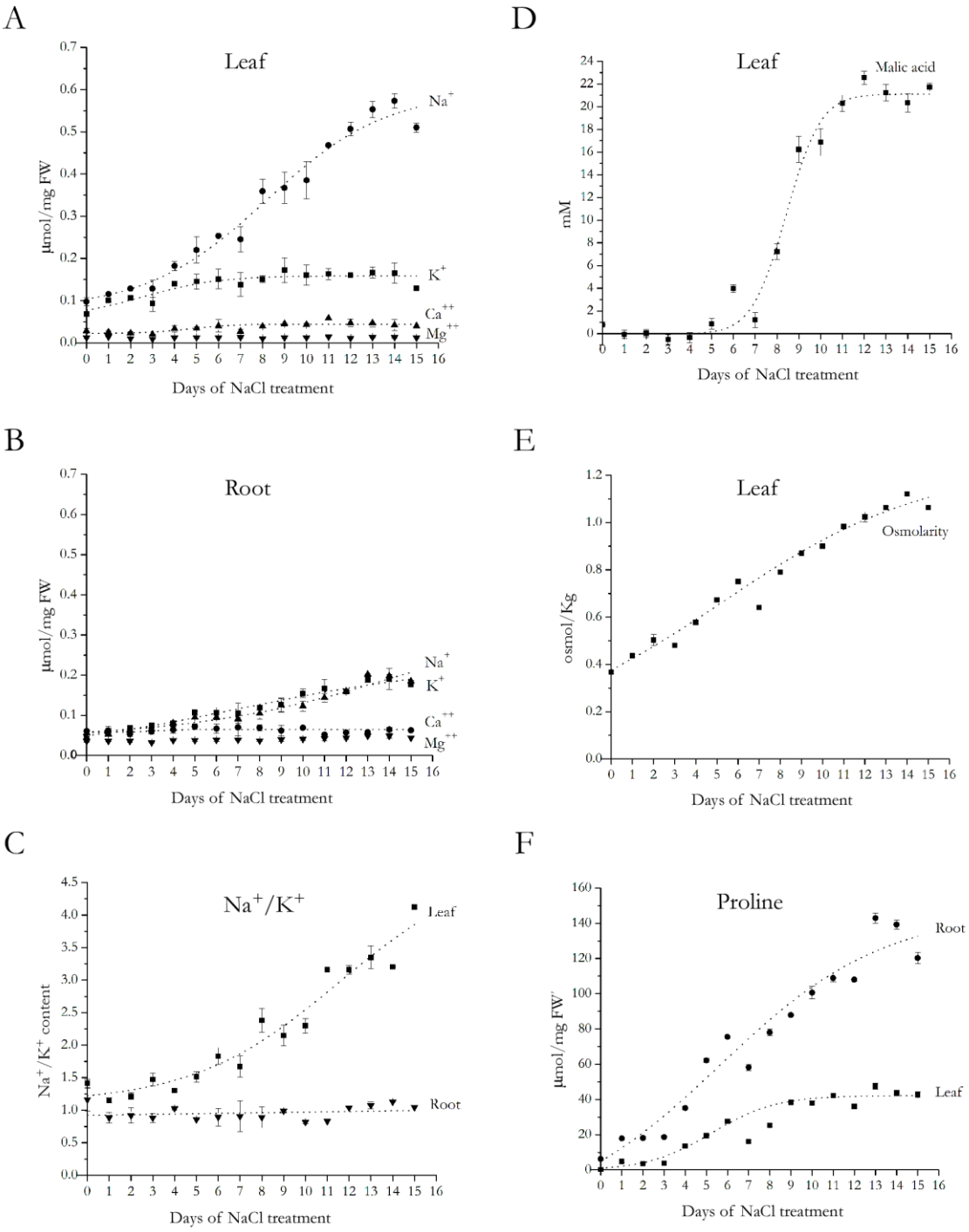

Figure 10. Physiological parameters of *Mesembryanthemum crystallinum* plants upon salt treatment. Time courses of Na^+ and K^+ accumulation in leaf (**A**) and root (**B**), Na^+/K^+ accumulation ratios (**C**), malic acid compartmentation (**D**) in leaves, leaf osmolarity (**E**) and proline storage (**F**) in leaf and root tissue. Plants were harvested at different days of NaCl treatment. Samples subjected to analyses were pooled from leaf and root tissue of three plants. Data represent mean values (n=3) ± SD and are fitted by the logistic curve [2].

Table 7. Summary of characteristic physiological parameters obtained by fitting data point s of individual analyses in Fig. 10 by a logistic equation [2]. R^2: Pearson's correlation coefficient; A_{max}: maximum concentration; $t_{1/2}$: time required to reach half of the maximum value

Tissue	Parameter	Concentration at saturation	$t_{1/2}$ (day)	R^2
Leaf	K^+	0.15±0.01 μmol/g FW	3.8±0.03	0.91
	Na^+	0.85±0.12 μmol/g FW	11.7±1.5	0.99
	Malic acid	21.3±0.4 mM	8.4±0.1	0.99
	Osmolarity	1.5±0.01 osmol/Kg	10.7±0.1	0.98
	Proline	54.1±0.9 μmol/gFW	7.4±0.1	0.97
Root	K^+	0.25±0.01 μmol/g FW	10.2±0.3	0.98
	Na^+	0.25±0.015 μmol/g FW	10.7±0.3	0.98
	Proline	213.7±27.70 μmol/g FW	11.3±1.8	0.98

Malate concentration approached saturation at day 10 to 12 indicating complete CAM induction only from day 12 on.

Comparison of the Na^+ and the malate data shows that accumulation of Na^+ starts about 4 days earlier than that of CAM. Malate accumulation indeed shows rather fast accumulation kinetics and reaches saturation over a period of 3 to 4 days. Compared to the accumulation of Na^+, malate accumulation starts much later than the accumulation of Na^+. Thus, nocturnal malate accumulation follows the increase in Na^+ accumulation in leaf cells with a lag of several days. Once plants were fully in the CAM state also the maximum day-night changes of malate accumulation were determined. The results of these measurements provide a difference in malate concentration of 21.3±0.4 mM. This value is in the same range of what has been reported previously for *M. crystallinum* plants cultivated under the same conditions (Broetto *et al.* 2002, Libik *et al.*, 2004).

Figure 10E shows the time course of leaf osmolarity over 15 days of NaCl stress. Curve fitting of data reveals a net increase in osmotic pressure of 1.5±0.01 osmol/kg with a $t_{1/2}$ of 10.7±0.1 days. The increase of leaf osmolarity reflects the accumulation of Na^+, K^+ and the synthesis of osmolytes such as proline (see below).

M. crystallinum plants exposed to high NaCl concentrations in the soil need to respond without much delay to changes of osmotic conditions in order to ensure the flux of water to the above ground plant organs. One strategy to conquer osmotic stress is to synthesise compatible osmolytes such as proline (Heun *et al.*, 1981, Demmig and Winter, 1986, Thomas *et al.,* 1992). As shown in Figure 10F proline was synthesised in leaf and in root cells in response to NaCl stress; data are in agreement with previous observations of Sanada and co-workers (1995) in *M. crystallinum* plants under salt stress. Proline was mainly accumulated in roots where the Na^+ accumulation was significantly lower than in leaves (see Fig. 10B). Thus the proline concentration of root cells at complete CAM induction was approximately 3.9 times higher than proline of leaf cells (Table 7). Moreover, proline accumulation in leaves occurred slower ($t_{1/2}$ 7.4±0.1 days) than in roots ($t_{1/2}$ 11.3±1.8 days) because in roots proline levels had to reach higher concentration levels.

In summary, the data demonstrate that the plants employed in the present study have endured an effective shift from C3 photosynthesis to CAM under high salinity. As expected the external salt stress elicited an osmotic reaction in leaf as well as in root cells in order to ensure the water flow up to the photosynthetic organs. For this purpose leaves accumulate more Na^+ than K^+. In roots both cations are accumulating at equivalent amounts keeping a steady Na^+/K^+ ratio. Mg^{++} and Ca^{++} did not show any significant response to NaCl stress in both leaves and roots tissues.

5.9 Compartmentation of Na^+ in mesophyll cells

The overall results reported above provide some information on the time course of Na^+ accumulation and compartmentalization in *M. crystallinum* at the tissue level. Previous results have already provided some insights into the accumulation of Na^+ on the cellular level and in particular on the level of vacuolar compartment (Epimashko *et al.*, 2004; Adams *et al.*, 1998). It was reported that the vacuoles of *M. crystallinum* can be differentiated into acidic and neutral types on the basis of their vacuolar acidity. In order to get an overview of Na^+ compartmentalization at the cellular level and in the context of the two different types of vacuoles leaf cross-sections of *M. crystallinum* have been stained with CoronNa green, a Na^+-sensitive fluorescent dye, and with Neutral Red, a pH-indicator dye that stains acidic cells in red. In leaf cross-sections of plants in which CAM metabolism has been induced by salt stress, Na^+ compartmentalization is distributed in a rather uniform manner across the entire section (Figure 11B).

The nature of the vacuoles on the other hand is not uniform across the sections.

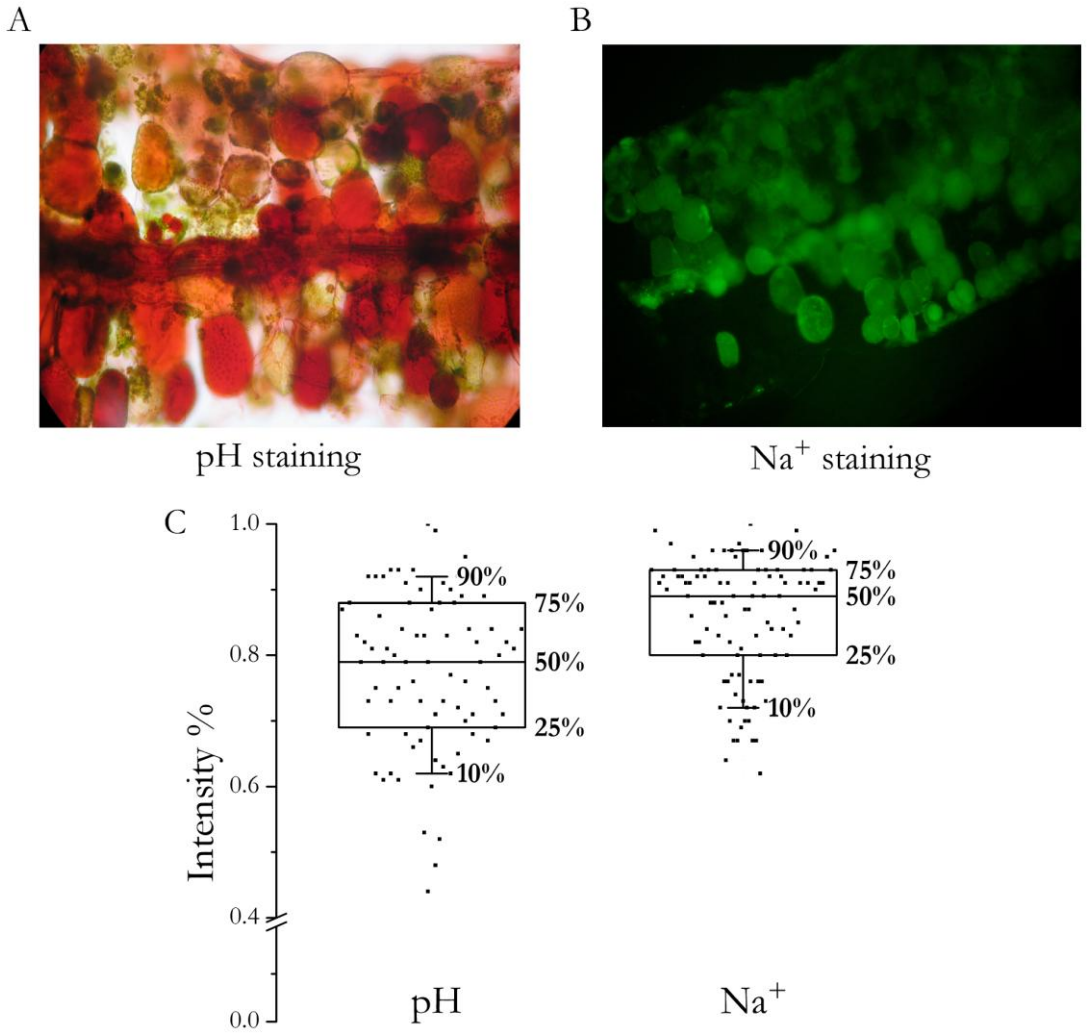

Figure 11. Leaf cross sections of *Mesembryanthemum crystallinum* plants performing CAM induced by NaCl treatment. (**A**) Neutral Red staining reveals different pH conditions across the tissue section. (**B**) CoroNa green straining shows a homogeneous accumulation of Na^+ ions in the tissue section. (**C**) Box chart distribution of the normalized intensities of pH and Na^+ staining in CAM plants induced by salt stress. The boxes indicate from the bottom the 25th, the 50th and the 75th percentiles of the distribution of the intensities. Upper and lower bars indicate the range comprising the 10th-90th percentiles (80% of the cells).

On the basis of the neutral red staining the cross-sections reveal two different types of vacuoles, an acidic (deep red) and a more neural (non-stained) vacuole (Figure 11A). To quantify the distribution of fluorescence and staining intensities 86 Neutral Red stained cells (from 6 leaf cross-sections) and 102 CoroNa green stained cells (from 9 leaf cross-sections) of CAM induced plants were analyzed. The normalized average of the staining intensities

between pH and Na^+ were quite similar, 0.78±0.12 and 0.83±0.13, respectively. In spite of that their distribution was different as reported in the box chart of Figure 11C. The 50th percentile of pH and Na^+ staining was calculated as 79% and 89% of the brightest intensity, respectively. However, 80% of the sampled cells displayed a relative intensity of Na^+ staining in the range between 0.72 and 0.96. In contrast with respect to pH, the range of relative intensity occupied by 80% of the cells was much broader between 0.62 and 0.92. These data become even more evident when considering the lower loading capacity of CoroNa green in respect of Neutral Red into the cells. Without this problem the relative fluorescence of the Na^+ signal may even be higher.

These data report that the variability of the intensities of the leaf cross-sections is higher in the case of pH staining instead of the Na^+ detection, suggesting a more uniform Na^+ accumulation distribution over a wider range of vacuolar pH.

Epimashko *et al.* (2004) suggested that two functionally different vacuoles in *M. crystallinum* mesophyll cells physically separate the two contrasting function of malic acid and Na^+ vacuolar accumulation. The above results, however, indicate that the pattern of pH distribution is neither positively nor negatively correlated with that of Na^+ accumulation. This implies that Na^+ can be found in vacuoles independently of their acidity.

In order to investigate Na^+ accumulation in vacuoles with different acidity, *M. crystallinum* plants were stressed with NaCl for 15 days. This time is sufficient to fully switch the plants from C3 photosynthesis to CAM metabolism (see Fig. 10D; Lüttge, 1993). Leaf cross-sections from these plants were stained first with CoroNa green and subsequently with Neutral Red. Figure 12 shows Na^+ accumulation (Fig. 12A) with respect of the acidity of the vacuoles (Figure 12B) in mesophyll cells.

CoroNa green staining is apparent in four cells indicating Na^+ accumulation (Figure 12A). The identical tissue sections have subsequently been stained with Neutral Red to monitor the acidity of the vacuoles. Figure 12B shows that two out of four Na^+ storing cells strongly accumulate Neutral Red, i.e. these cells are highly acidic. One out of four cells reveals only a small neutral red accumulation indicating a neutral pH. The results of this representative experiment implies that Na^+ accumulating vacuoles can be both acidic and neutral (red and yellow circles, respectively, in Fig. 12). The same results were obtained in other experiments: in a total of 33 Na^+ accumulating cells of M. *crystallinum* plants in CAM state 14 (43%) were found to be acidic while 19 (57 %) exhibited a neutral vacuole. This situation changed slightly in cells from plants in C3 state. Here 13 Na^+ accumulating cells were observed in which 4 (31%) cells had an acidic and 9 (69%) a neutral vacuole. A comparison between

CAM and C3 plants shows that the ratio between acidic and neutral vacuoles for Na^+ accumulating cells increases in CAM leaves compared to C3.

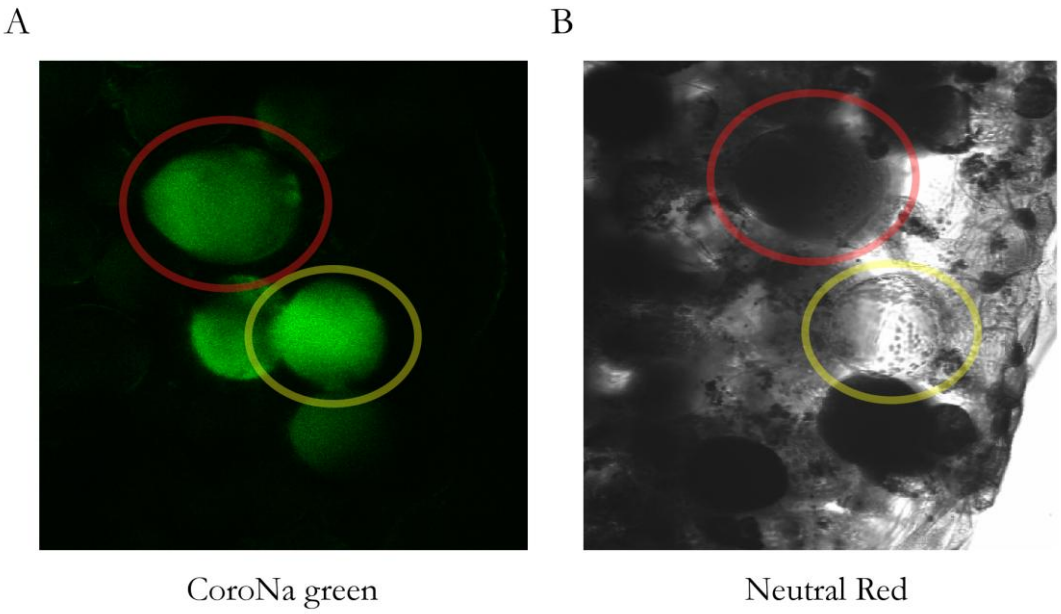

Figure 12. Na^+ accumulates in acidic as well as in neutral vacuoles of leaf mesophyll cells of salt stressed *M. crystallinum*. Plants were treated with NaCl for 15 days and performed CAM. Leaf cross sections were sequentially stained with CoroNa green (**A**) and neutral red (**B**); acidic vacuoles and neutral vacuoles appear in dark and pale-grey to unstained, respectively; Na^+ accumulating vacuoles show green fluorescence; identical vacuoles in **A** and **B** are marked by corresponding colours.

In conclusion, these data reveal that vacuoles characterized by storing Na^+ to a lower or higher extent can be found throughout the mesophyll of salt treated *M. crystallinum* plants. These vacuoles do not function exclusively in Na^+ storage because they also accumulate malic acid which moves the inner vacuolar compartment to a more acidic pH. So the Na^+ and malic acid storage functions are not completely separated: nonetheless there seems to be a preference in storing one or the other.

6 Discussion

Plant nutrition depends on the activity of membrane transporters that translocate minerals from the soil into the plant and mediate their intra- and intercellular distribution. The genome of *A. thaliana* appears to encode more than 800 membrane transport proteins, 65% of which are secondary active transporters (Pardo *et al.*, 2006). In plants most co-transporters are energized by the H^+ electrochemical gradient generated by primary proton pumps working in all cellular membranes but alternative couplings also exist.

Uptake and translocation of cations play essential roles in plant nutrition, signal transduction, growth and development. The focus of the present work has been Na^+ because it is a principal component of the deleterious effects associated with salinity stress. Mechanisms of Na^+ transport were investigated in the facultative halophyte *M. crystallinum* which is a model system for studying adaptation to environmental stresses including salt stress in higher plants (Winter, 1973; Lüttge, 1993). Under salt stress this plant accumulates Na^+ in order to adjust to the new osmotic condition; simultaneously it switches from C3 photosynthesis to CAM.

Given the negative membrane potential difference at the plasma membrane of plants (Higinbotham, 1973) a rise in extra-cellular Na^+ concentration establishes a large electrochemical gradient favoring the passive transport of Na^+ into the cells. Pioneering studies conducted by Epstein (1973) demonstrated that Na^+ competes with K^+ for uptake by plant roots implying that K^+ transporters are also the gates for Na^+ entry. Three different low-affinity K^+ channels have been identified that can also mediate passive Na^+ uptake into the cell: (1) inward rectifying K^+ channels (KIRC) such as AKT1, catalyze K^+ influx at hyperpolarized membrane potentials and they display a high K^+/Na^+ selectivity ratio (Sentenac *et al.*, 1992); (2) outward rectifying channels (KORCs) which open during the depolarization of the plasma membrane and can mediate the efflux of K^+ and the influx of Na^+ ions (Maathuis and Sanders, 1995); (3) voltage-independent, non-selective cation channels (NSCC) have a relatively low Na^+/K^+ selectivity, are not gated by voltage and provide a pathway for the entry of Na^+ into plant cells (Maathuis and Amtmann, 1999). In addition, Na^+ ions can also enter the cell through several low- and high-affinity K^+ carriers. Among these, HKT1 has been shown to function as selective Na^+ transporters rather than mediating a high-affinity K^+ translocation (Uozumi et al., 2000). Berthomieu et al. (2003) proposed that AtHKT1 from *A. thaliana* mediates Na^+ loading into the leaf phloem and Na^+ unloading from the root phloem sap and thus plays a key role in long-distance Na^+ transport

and Na^+ circulation in the plant. In *M. crystallinum* McHKT1 localizes to the plasma membrane of leave cells and its expression increases upon salt stress (Su et al., 2003).

Under physiological conditions plants maintain a high cytosolic K^+/Na^+ ratio by extruding Na^+ ions out of the cell or compartmentalizing them into the vacuole (Blumwald, 1987; Apse *et al.*, 1999). This becomes especially important when plants are exposed to high salinity. Proteins that play a primary role in this homeostatic mechanism are the Na^+/H^+ antiporters. Na^+/H^+ antiporters are membrane proteins that exchange Na^+ for H^+. They couple the transport of Na^+ against the electrochemical gradient to the movement of H^+ down the electrochemical gradient. They were discovered in *E. coli* by West and Mitchell (1974). As expected from their central role in pH and Na^+ homeostasis (Padan *et al.*, 2001) they were subsequently found to be widely spread throughout the biological kingdom from bacteria to mammals including humans.

A major cellular compartment for Na^+ accumulation in plants is the central vacuole (Apse *et al.*, 1999). Vacuolar sequestration of Na^+ ions occurs via Na^+/H^+ antiporters at the tonoplast (Blumwald, 1987; Apse *et al.*, 1999). These proteins belong to the IC-NHE/NHX family. However, recent advances indicated that in addition to functioning at the vacuolar membrane they can also work at endosomal membranes. In this respect they can play a critical role in K^+ homeostasis, luminal pH control, and vesicle trafficking (Pardo *et al.*, 2006).

Until now only little information was available about Na^+/H^+ antiporters in *M. crystallinum*. (Barkla et al., 1995; Chauhan et al., 2000; Barkla et al., 2002; Epimashko et al., 2006). The five Na^+/H^+ antiporters cloned in this study now provide a new basis for a more complete picture of salt adaptation of *M. crystallinum*.

The cloned McNHX1 transporter shows high sequence similarity to the two vacuolar Na^+/H^+ antiporters AtNHX1 and AtNHX2 from Arabidopsis (Yokoi *et al.*, 2002), 74.6% and 76.6% respectively. This suggests that it moves Na^+ ions from the cytoplasm to the vacuolar lumen. The hypothesis is further supported by the observation that McNHX1 complements the yeast mutant *nhx1* against hygromycin B selection and that its expression level increases upon salt stress. In contrast McNHX3 shows only 57.5 % of similarity with McNHX1 and it does not complement the yeast mutant *nhx1* upon hygromycin B selection. However, McNHX3 belongs to the class I of the IC-NHE/NHX antiporters as for McNHX1 and AtNHX1. These findings, together with the fact that AtNHX1 has been found to co-localize with V-ATPase in tonoplast as well as Golgi/endoplasmic reticulum enriched membrane fractions of *A. thaliana* (Apse *et al.*, 1999), strongly suggest a possible

role of McNHX3 in pre-vacuolar Na^+ compartmentalization. Similarly McNHX2 is supposed to accumulate Na^+ into compartments of the endomembrane system since its high similarity with AtNHX5-6 (71% and 75.7%, respectively), as previously proposed for AtNHX5 (Pardo *et al.*, 2006). The hypothesis that Na^+ accumulation into pre-vacuoles and endosomal compartments plays a role in adaptation to salt stress in *M. crystallinum* is furthermore supported by the fact that the level of the V-ATPase E subunit was found increasing upon salt stress in the endosomal compartments of *M. crystallinum* (Golldack and Dietz, 2001).

The cloned McSOS1 antiporter has been demonstrated to complement *nha1 nhx1* yeast mutant and shows 61.4 % of sequence similarity to the plasma membrane Na^+/H^+ antiporter AtSOS1 and even a higher similarity with other halophyte NhaP/SOS1 transporters. It is thus supposed to mediate the Na^+ extrusion from the cell across the plasma membrane.

Finally, the McNhaD antiporter cloned in the present study most likely mediates the accumulation of Na^+ into chloroplasts of *M. crystallinum*. McNhaD complements *nha1 nhx1* yeast mutants in a way similar to McSOS1. At the same time it complements the *nhaA nhaB E. coli* mutant at both 5.5 and 7.5 pH in the medium.

Similar functional complementation tests were previously performed with PeNhaD1 (Ottow *et al.*, 2005), an IT/NhaD type antiporter from *Populus euphratica*, but only cells at pH 5.5 were able to grow. The same pH-dependence was also observed for the VcNhaD exchanger of *Vibrio cholerae* (Dzioba *et al.*, 2002). The comparison of the current results with those obtained from *P. euphratica* studies performed at pH 5.5 indicates similar growth rates for the control cells carrying empty vectors and similar recovery rates under LiCl conditions (80% of recovery for McNhaD and 78% for PeNhaD). Instead McNhaD complementation showed a lower recovery rate in NaCl (56% of the untreated control) with respect to PeNhaD1 (80%). In any case, in contrast to PeNhaD1, McNhaD has been able to complement the *nhaA nhaB E. coli* mutant also at pH 7.5, up to 40% for NaCl and 29% for LiCl treatments with respect to the untreated control (Figure 6 and Table 5).

In summary, McNhaD complements the *nhaA nhaB E. coli* Na^+ sensitive mutant similarly to PeNhaD1. Only when cells were treated with 200 mM NaCl McNhaD generated a lower rate of recovery than PeNhD1. Also in contrast to PeNhaD1, McNhaD can complement the *nhaA nhaB E. coli* mutant not only at an acidic pH but also at pH 7.5 in the medium. The ability of McNhaD in maintaining the recovery of the growth from Na^+ inhibition at pH 7.5 suggests that this protein acts as a high affinity antiporter on Na^+ extrusion being antiporter

able to offer protection against toxic alkali cations even with a low H^+ gradient across the membrane.

When transiently expressed in *V. faba* stomata guard cells McNhaD localizes at the chloroplast membrane. This finding is in agreement with the localization in chloroplast membranes of PpNhaD1, the IT/NhaD exchanger of *Physcomitrella patens* (Barrero-Jil *et al.*, 2007). The McNhaD transcript levels increase upon salt stress of *M. crystallinum* and this increment is accompanied by a Na^+ accumulation into chloroplasts. All these observations strongly support the idea the McNhaD is the main pathway responsible for Na^+ transport into the plastidial compartment. One may speculate that chloroplasts need to accumulate Na^+ in order to ensure a quick osmotic balance with respect of the altered osmotic conditions in the cytoplasm under salt stress. The increase of McNhaD transcript levels correlates with the observed kinetic of Na^+ accumulation into chloroplasts. They both start to increase at about day 4 of the salt treatment. These findings are in agreement with previous observations by Demming et al. (1986) who reported high Na^+ concentrations in chloroplasts reaching values of up to 156-234 mM in isolated chloroplast of NaCl treated *M. crystallinum* plants. However, until now the transporters responsible for Na^+ accumulation have not been identified. The present work reports the first evidence for a direct involvement of a plastidial Na^+/H^+ antiporter in the Na^+ accumulation into these organelles. The data reported in this study do not let discriminate at which chloroplast membrane the McNhaD antiporter localizes. However, because many important biochemical processes occurring in the stroma compartment are Na^+ sensitive, it is unlikely to suppose that Na^+ is accumulated in the stroma. Rather it may be accumulated in the lumen of the thylakoid membranes. In effect the high H^+ concentration of thylakoids achieved by the activity of the photosynthetic electron transport may active the antiport with Na^+ ions in order to mediate their Na^+ accumulation. On the other hand if McNhaD mediates Na^+ transport into thylacoids, one would expect to see a co-localization of McNhaD:GFP and chlorophyll fluorescence inside chloroplast and not only chlorophyll fluorescence surrounded by McNhaD:GFP. The actual localization and exact function of McNhaD transporter remains to be shown.

However, at the chloroplast level McNhaD may contribute to the mechanisms which regulate the osmotic condition in and Na^+ detoxification of the stroma as the IC-NHE/NHX and NhaP/SOS1 antiporters are supposed to do at the cytosol.

To determine the role of the individual transporter the expression level and Na^+ accumulation were analyzed in leaves and roots. The cloned antiporters McNHX1, McSOS1

and McNhaD are up-regulated by Na^+ stress in leaves and are therefore likely involved in the salt stress adaptation mechanism of *M. crystallinum*. The data imply that vacuolar and chloroplast Na^+ storage and Na^+ export across the plasma membrane are much more important in leaves than in roots since the transcript levels of these antiporters were only up-regulated in leaves but not in roots. Na^+-insensitive induction of the expression of the Na^+/H^+ antiporters in roots is compensated for the strong up-regulation of McITS1, a Na^+/*myo*-inositol symporters that transfers sodium from the root cells to the leaf mesophyll as a halophytic strategy that lowers the osmotic potential (Chauhan *et al.*, 2000).

The present data demonstrate that Na^+ accumulation in the leaves of *M. crystallinum* is a fast response starting from about day 4 of NaCl treatment. This is several days before the transition to CAM occurs as indicated by malate accumulation during the night. Early Na^+ accumulation may be a strategy to give an immediate answer to the changed osmotic conditions. Only in a second step the transition from C3 photosynthesis to CAM occurs in order to assure an efficient energy-conserving metabolism (Lüttge, 1993; Niewiadomska *et al.*, 2004). In *M. crystallinum* an ABA-induced V-ATPase activity may be linked to the stress-induced, developmentally programmed switch from C3 metabolism to CAM metabolism in adult plants. However, in the case of vacuolar Na^+ sequestration, energized by the V-ATPase and mediated by Na^+/H^+ antiport activities, ABA-independent pathways are involved (Barkla *et al.*, 1999).

To quantify the correlation between increase in transcript levels of Na^+/H^+ antiporters and Na^+ accumulation in mesophyll cells the original data where further analyzed. Figure 13 reports a model of the direct temporal coincidence between Na^+ and K^+ compartmentalization in leaf and the rise in McNHX1 transcripts. The first derivative slope indicates how quick the stress induced kinetic of the ion accumulation is. Instead the second derivative points out the starting and the ending points of the stress induced rise of gene expression at the higher and lower peak, respectively; moreover the intersection of x-axis represents the point of the maximum speed of expression and the asymptotic approximation to the x-axis indicates that gene expression is reaching the final saturation.

The model assumes that an induction stimulus occurs at days 2 of NaCl treatment. Following that assumption the beginning of McNHX1 transcript expression occurs around day 3 of NaCl stress. This is also the time when Na^+ and K^+ start quickly to accumulate in leaf cells. The plateau of the K^+ derivative slope indicates that the accumulation process of that ion already reached the final saturation at day 5, i.e. the cellular concentration of K^+ does not increase any longer. However at day 5 the expression of McNHX1 is still

increasing and has just only passed the maximum increment point, coinciding in between day 4 and 5. At the same time the Na^+ accumulation rate increases in a linear fashion from day 5 up to around day 10. This is in agreement with the second derivative of McNHX1 expression which indicates that the gene expression is reaching the final saturation only at day 10. The second derivative slopes of the expression of the other antiporters are also reported in Figure 13. However, their kinetic does not correlate with the Na^+ accumulation as above explained for McNHX1.

In summary these observations support the view that McNHX1 is responsible for the vacuolar Na^+ compartmentation in leaves, the main Na^+ storage compartment of the cell. The selectivity of McNHX1 for Na^+ appears to be much higher than for K^+ since K^+ is not accumulated anymore although McNHX1 is at the maximum rate of increase of transcript level; accordingly also the cellular concentration of Na^+ is still increasing.

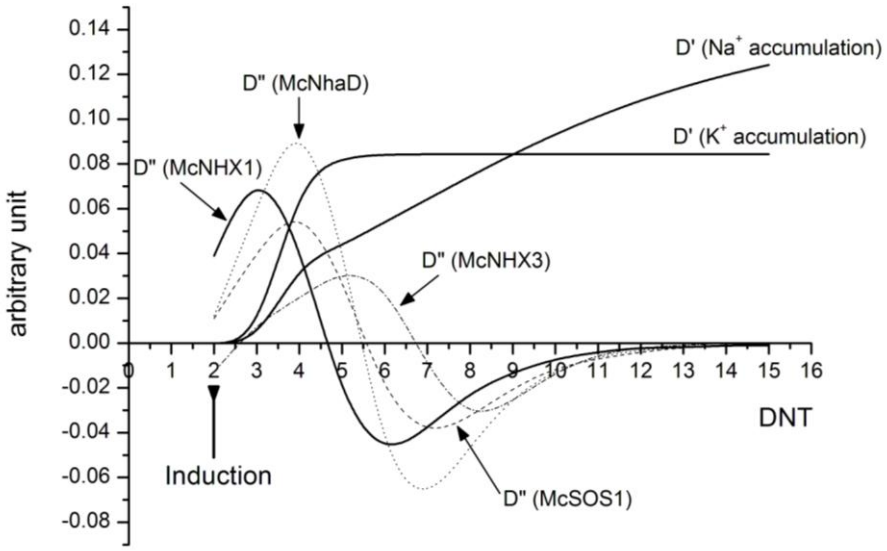

Figure 13. McNHX1 is the main responsible for Na^+ accumulation in mesophyll cells. First derivatives (**D'**) of K^+ and Na^+ time curse accumulation curves in leaves have been compared with the second derivatives (**D"**) of Na^+/H^+ antiporter time curse expression curves in leaves. When McNHX1 is still at $t_{1/2}$ of the saturation transcript level, K^+ accumulation is not increasing anymore, while the kinetic of Na^+ accumulation becomes linear up to the maximum of McNHX1 transcript level. That is the time when its second derivative slope approximates to zero and the transcript level is approaching to saturation.

Not all the cloned antiporters have been proved to be up-regulated upon NaCl stress. McNHX2 has not been detectable, probably because of a very low basal expression level. Moreover McNHX3, even though it was detectable, did not show any appreciable increment

upon NaCl treatment with respect to the condition prior to salt treatment. McSOS1, which has been demonstrated to complement *nha1 nhx1* yeast mutant and which shows a high similarity to AtSOS1, reacts in response to NaCl stress by increasing its transcript levels. Hence it can be assumed that McNHX1 contributes to vacuolar Na^+ sequestration and its expression increase upon salt stress; McNHX2 and McNHX3 are supposed to transport Na^+ ions into small vesicles and, in particular, the expression of McNHX3 may be only slightly associated with salt adaptation; McNHX2 instead is low expressed in leaves as well as in roots. McSOS1 operates in order to extrude the excess of cytoplasmic Na^+ ions; McNhaD has been surprisingly found to be involved in Na^+ accumulation in chloroplasts.

The present data show that several cellular compartments are involved in the rapid osmotic adjustment and cytoplasm detoxification mechanism that occurs in *M. crystallinum* starting at 3 to 4 days after initiation of NaCl stress. The time course quantifications reported here at tissue level suggest that the Na^+ sequestration occurs much earlier than the shift of C3 photosynthesis to CAM, highlighted by the time course of vacuolar malate accumulation (Fig. 10A and 10D). This observation confirms that the Na^+ accumulation is a short term adaptation mechanism that occurs before the long term adaptation mechanism that shifts cells to CAM metabolism. However, on the cellular level no clear distinction can be made between malic acid and Na^+ accumulating cells. Figure 11 indicates in agreement with a previous study (Epimashko *et al.*, 2004) that mesophyll cells of *M. crystallinum* have vacuoles with different pH. Also these mesophyll cells reveal a different capacity of Na^+ accumulation. However, the simultaneous recording of pH and Na^+ accumulation exhibits no apparent correlation between these two parameters. Such a correlation would have been expected if Na^+ accumulation and malic acid compartmentalization were exclusively occurring in one or the other type of vacuole. The observation that CAM metabolism follows Na^+ accumulation with such a long temporal delay however makes it rather unlikely that the two functions are really separated in two distinctly different types of vacuoles. The data rather show a preference of vacuoles for Na^+ over malic acid accumulation but not a clear separation of function. Na^+ compartmentalization seems to be more homogeneously distributed over the entire mesophyll than the acidity of the vacuoles (Fig. 11; Epimashko *et al.*, 2004). Therefore it seems plausible to assume that all mesophyll cells of *M. crystallinum* participate in the early Na^+ sequestration, as well as in the malic acid accumulation once CAM metabolism starts, without any specific differentiation. The halophyte *M. crystallinum* accumulates high quantities of Na^+ into vacuoles, as well as other inner organelles, for instance chloroplasts, in order to allow immediate detoxification of the cytoplasm from Na^+.

In contrast, proline synthesis supports the osmotic cellular re-adaptation mainly in roots; instead Na^+ is removed from roots, where the ratio with K^+ does not change upon NaCl treatment, and stored in leaf cells.

The data obtained in this study can be included in a model for salt adaptation in *M. crystallinum* on the cellular level (Fig. 14). Together with already known transporters the cloned Na^+/H^+ antiporters provide a more complete insight into the pathway of Na^+ sequestration upon salt stress.

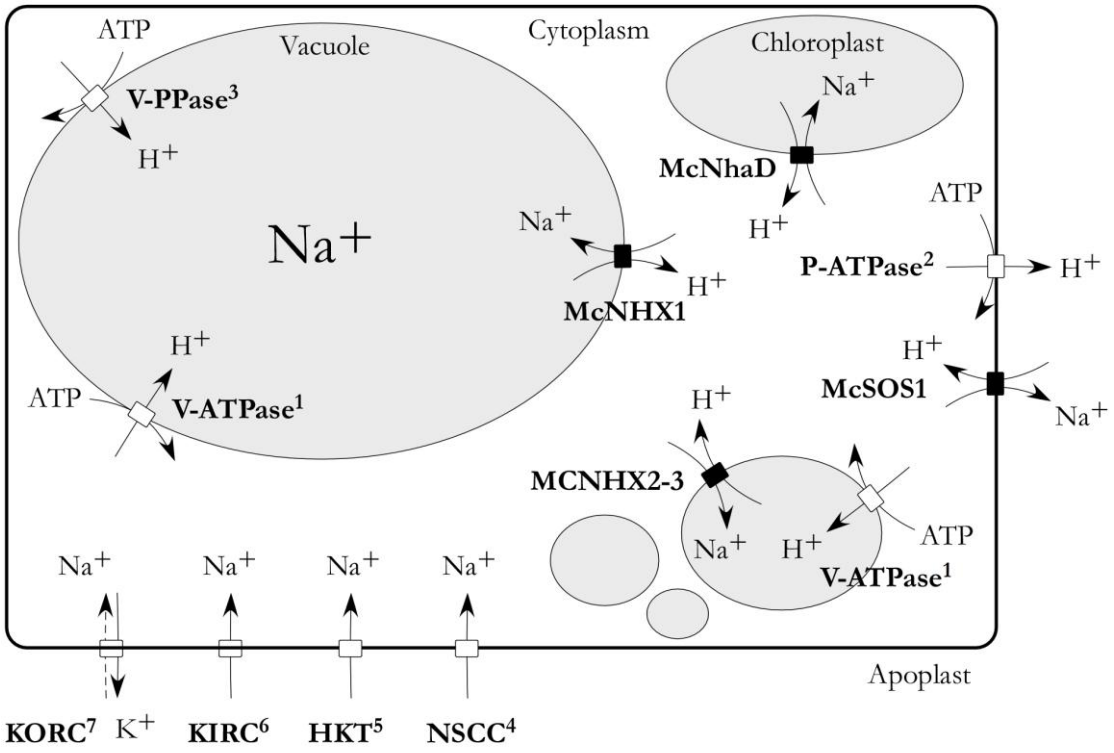

Figure 14. Model summarizing the Na^+ uptake mechanisms in *Mesembryanthemum crystallinum*. (**1**) V-ATPase: vacuolar H^+-ATPase (Barkla *et al.*, 1995); (**2**) P-ATPase: plasma membrane H^+-ATPase (Vera-Estrella *et al.*, 1999); (**3**) V-PPase: vacuolar H^+-pyrophosphatase (Bremberger *et al.*, 1988); (**4**) NSCC: voltage-independent, non-selective cation channels that have a relatively high Na^+/K^+ selectivity and provide a pathway for the entry of Na^+ into plant cells (Maathuis *et al.*, 1999); (**5**) HKT: selective Na^+ transporter and, to a lesser extent, mediator of K^+ transport (Uozumi *et al.*, 2000); (**6**) KIRC: inward rectifying channels, such as AKT1 (Sentenac *et al.*, 1992); (**7**) KORC: inward rectifying channels that could mediate the efflux of K^+ and the influx of Na^+ ions (Maathuis *et al.*, 1995). The Na^+/H^+ antiporters characterized in the present study are reported as black squares.

The reported data show that Na^+ can also be stored into chloroplast at high concentrations and it is correlated with the increased expression of the plastidial Na^+/H^+ antiporter, McNhaD.

These studies contribute to our understanding on how plants cope with excessive Na^+ in the environment. This topic is even more becoming of great agricultural importance as soil salinity accounts for large yield losses in crops worldwide. Further physiological analyses and the coupling of the activity of aquaporins and proton pumps with the current characterized Na^+/H^+ antiporters will be required to provide a more clear overview of the Na^+ accumulation mechanisms in the adaptation to saline stress of the halophyte *M. crystallinum*.

7 Acknowledgments

We thank Cristina Bonza, University of Studies of Milan, for providing the plant GFP expression vector pUC19:GFP; Adam Bertl, Technische Universität Darmstadt, for providing strains and precious suggestions in working with yeast mutants; Thomas Teichmann, University of Giessen, for providing the EP432 *E. coli* mutant and pQE60 expression vector; Francesca Sparvoli, IBBA-CNR Institute of Milan, for providing real time PCR instrumentation support. The project was carried out in the framework of the Graduatenkolleg 340 "Communication in biological systems: from the molecule to the organism in its environment".

8 References

Adams, P., Nelson, D.E., Yamada, S., Chmara, W., Jensen, R.G., Bohnert, H., and Griffiths, H. (1998). Growth and development of *Mesembryanthemum crystallinum*. New Phytol. **138**, 171-190.

Agarie, S., Shimoda, T., Shimizu, Y., Baumann, K., Sunagawa, H., Kondo, A., Ueno, O., Nakahara, T., Nose, A., and Cushman, J.C. (2007). Salt tolerance, salt accumulation, and ionic homeostasis in an epidermal bladder-cell-less mutant of the common ice plant *Mesembryanthemum crystallinum*. J. Exp. Bot. **58**, 1957-1967.

Apse, M.P., Aharon, G.S., Snedden, W.A., and Blumwald, E. (1999). Salt tolerance conferred by overexpression of a vacuolar Na^+/H^+ antiport in *Arabidopsis*. Science **285**, 1256-1258.

Apse, M.P., and Blumwald, E. (2007). Na^+ transport in plants. FEBS Letters **581**, 2247-2254.

Arnon, D.I. (1949). Copper enzymes in isolated chloroplasts. Polyphenol oxidase in *Beta vulgaris*. Plant Physiol. **24**, 1-15.

Barkla, B.J., Zingarelli, L., Blumwald, E., and Smith, A.C. (1995). Tonoplast Na^+/H^+ antiport activity and its energization by the vacuolar H^+-ATPase in the halophytic plant *Mesembryanthemum crystallinum* L. Plant Physiol. **109**, 549-556.

Barkla, B.J., Vera-estrella, R., Maldonado-Gama, M., and Pantoja, O. (1999). Abscisic acid induction of vacuolar H^+-ATPase activity in *Mesembryanthemum crystallinum* is developmentally regulated. Plant Physiol. **120**, 811-819.

Barkla, B.J., Vera-estrella, R., Camacho-Emiterio, J., and Pantoja, O. (2002). Na^+/H^+ exchange in the halophyte *Mesembryanthemum crystallinum* is associated with cellular sites of Na^+ storage. Funct. Plant Biol. **29**, 1017-1024.

Barrero-Gil, J., Rodriguez-Navarro, A., and Benito, B. (2007). Cloning of the PpNHAD1 transporter of *Physcomitrella patens*, a chloroplast transporter highly conserved in photosynthetic eukaryotic organisms. J. Exp. Botany **58**, 2839-2849.

Bates, L.S. (1973). Rapid determination of free proline for water-stress studies. Plant and Soil **39**, 205-207.

Berthomieu, P., Conéjéro, G., Nublat, A., Brackenbury, W.J., Lambert, C., Savio, C., Uozumi, N., Oiki, S., Yamada, K., Cellier, F., Gosti, F., Simonneau, T., Essah, P.A., Tester, M., Véry, A.A., Sentenac, H., and Casse, F. (2003). Functional analysis

of AtHKT1 in *Arabidopsis* shows that Na^+ recirculation by the phloem is crucial for salt tolerance. EMBO J. **22**, 2004–2014.

Binzel, M.L., and Ratajczak, R. (2001). Function of membrane transport systems under salinity: tonoplast. In: Läuchli, A., and Lüttge, U., eds. Salinity: environments – plants – molecules. Dordrecht: Kluver.

Blumwald, E. (1987). Tonoplast vesicles as a tool in the study of ion transport at the plant vacuole. Physiol. Plant. **69**, 731-734.

Blumwald, E. (2000). Sodium transport and salt tolerance in plants. Curr. Opin. Cell Biol. **12**, 431-434.

Bohnert, H.J., and Cushman, J.C. (2000). The ice plant cometh: lessons in abiotic stress tolerance. J. Plant Growth Regul. **19**, 334-346.

Bremberger, C., Haschke, H.P., and Lüttge, U. (1988). Separation and purification of the tonoplast ATPase and pyrophosphatase from plants with consitutive and inducible Crassulacean acid metabolism. Planta, **175**: 465-470.

Broetto, F., Lüttge, U., and Ratajczak, R. (2002). Influence of light intensity and salt-treatment on mode of photosynthesis and enzymes of the antioxidative response system of *Mesembryanthemum crystallinum*. Funct. Plant Biol. **29**, 13-23.

Chauhan, S., Forsthoefel, N., Ran, Y., Quigley, F., Nelson, D.E., and Bohnert, H.J. (2000). Na^+/*myo*-inositol symporters and Na^+/H^+-antiport in *Mesembryanthemum crystallinum*. Plant J. **24**, 511-522.

Cushman, J.C., and Bohnert, H.J. (1999). Crassulacean acid metabolism: Molecular Genetics. Ann. Rev. Plant Physiol. Plant Mol. Biol. **50**: 305–332.

Cushman, J.C., Tillett, R.L., Wood, J.A., Branco, J.M., and Schlauch, K.A. (2008). Large-scale mRNA expression profiling in the common ice plant, *Mesembryanthemum crystallinum*, performing C3 photosynthesis and Crassulacean acid metabolism (CAM). J. Exp. Bot., **59**: 1875-1894.

Darley, C.P., van Wuytswinkel, O.C.M., van del Woude, K., Mager, W.H., and de Boer, A.H. (2000). *Arabisopsis thaliana* and *Saccharomyces cerevisiae* NHX1 genes encode amyloride sensitive electroneutral Na^+/H^+ exchangers. Biochem. J. **351**, 241-249.

Demmig, B., and Winter, K. (1983). Photosynthetic characteristics of chloroplasts isolated from *Mesembryanthemum crystallinum* L., a halophilic plant capable of Crassulacean acid metabolism. Planta **159**, 66-76.

Demmig, B., and Winter, K. (1986). Sodium, potassium, chloride and proline concentrations of chloroplasts isolated from a halophyte, *Mesembryanthemum crystallinum* L. Planta **168**, 421-426.

Dietz, K.J., Tavakoli, N., Kluge, C., Mimura, T., Sharma, S.S., Harris, G.C., Chardonnens, A.N., and Golldack, D. (2001). Significance of the V-type ATPase for the adaptation to stressful growth conditions and its regulation on the molecular and biochemical level. J. Exp. Bot. **52**, 1969-1980.

Duy, D., Wanner, G., Meda, A.R., von Wirén, N., Soll, J., and Philippar, K. (2007). PIC1, an ancient permease in Arabidopsis chloroplasts, mediate iron transport. Plant Cell, **19**: 986-1006

Dzioba, J., Ostroumov, E., Winogrodzki, A. and Dibrov, P. (2002). Cloning, functional expression in *Escherichia coli* and primary characterization of a new Na^+/H^+ antiporter, NhaD, of *Vibrio cholerae*. Mol. Cell. Biochem. **229**, 119–124.

Epimashko, S., Meckel, T., Fischer-Schliebs, E., Lüttge, U., and Thiel, G. (2004). Two functionally different vacuoles for static and dynamic purposes in one plant mesophyll leaf cell. Plant J. **37**, 294-300.

Epimashko, S., **Fischer-Schliebs, E., Christian, A.L., Thiel, G., and Lüttge, U.** (2006). Na^+/H^+-transporter, H^+-pumps and an aquaporin in light and heavy tonoplast membranes from organic acid and NaCl accumulating vacuoles of the annual facultative CAM plant and halophyte *Mesembryanthemum crystallinum* L. Planta **224**, 944-951.

Epstein, E. (1973). Mechanisms of ion transport through plant cell membranes. Int. Rev. Cytol. **34**, 123-167.

Fukuda, A., Nakamura, A., Tagiri, A., Tanaka, K., Miyao, A., Hirochika, H., and Tanaka Y. (2004). Function, intracellular localization and the importance in salt tolerance of a vacuolar Na^+/H^+ antiporter from rice. Plant Cell Physiol. **45**, 146-159.

Garciadeblàs, B., Haro, R., and Benito, B. (2007). Cloning of two SOS1 transporters from the seagrass *Cymodocea nodosa*. SOS1 transporters from Cymodocea and Arabidopsis mediate potassium uptake in bacteria. Plant Mol. Biol. **63**, 479-490.

Gaxiola, R.A., Rao, R., Sherman, A., Grisafi, P., Alper, S.L., and Fink, G.R. (1999). The *Arabidopsis thaliana* transporters, AtNHX1 and Avp1, can function in cation detoxification in yeast. Proc. Natl. Acad. Sci. USA **96**, 1480-1485.

Gietz, R.D., and Schiestl, R.H. (1995). Transforming yeast with DNA. Methods Mol. Cell. Biol. **5**, 255–269.

Golldack, D., and Dietz, K.J. (2001). Salt-induced expression of the vacuolar H^+-ATPase in the common ice plant is developmentally controlled and tissue specific. Plant Physiol. **125**, 1643-1654.

Golldack, D. (2003). Molecular responses of halophyte to high salinity. Progr. Botany **65**, 219-234.

Harel-Bronstein, M., Dibrov, P., Olami, Y., Pinner, E., Schuldiner, S., and Padan, E. (1995). MH1, a second-site revertant of an *Escherichia coli* mutant lacking Na^+/H^+ antiporters (ΔnhaA ΔnhaB), regains Na^+ resistance and a capacity to excrete Na^+ in a $\Delta\mu M^+$-independent fashion. J. Biol. Chem. **270**, 3816-3822.

Hasegawa, P.M., Bressan, R.A., Zhu, J.K., and Bohnert, H.J. (2000). Plant cellular and molecular responses to high salinity. Annu. Rev. Plant Physiol. Plant Mol. Biol. **51**, 463-499.

Herz, K., Vimont, S., Padan, E., and Berche, P. (2003). Roles of NhaA, NhaB, and NhaD Na^+/H^+ antiporters in survival of *Vibrio cholerae* in a saline environment. J. Bacter. **185**, 1236–1244.

Heun A. M., Gorhan J., Lüttge U. and Wyn Jones R. G. (1991). Changes of water-relation characteristics and levels of organic cytoplasmic solutes during salinity induced transition of *Mesembryanthemum crystallinum* from C3-photosynthesis to crassulacean acid metabolism. *Oecologia* **50**, 66–72.

Higgins, D.G., Thompson, J.D., and Gibson, T.J. (1994). CLUSTAL W: improving the sensitivity of progressive multiple sequence alignment through sequence weighting, position-specific gap penalties and weight matrix choice. Nucleic Acid Res. **22**, 4673-4680.

Higinbotham, N. (1973). Electropotentials of plant cells. Annu. Rev. Plant Physiol. Plant Mol. Biol. **24**, 25–46.

Huson, D.H., and Bryant, D. (2006). Application of phylogenetic networks in evolutionary studies. Mol. Biol. Evol. **23**, 254-267.

Kagami, T., and Suzuki, M. (2005). Molecular and functional analysis of a vacuolar Na^+/H^+ antiporter gene of *Rosa hybrida*. Genes genet. Syst. **80**, 121-128.

Kholodova, V.P., Neto, D.S., Meshcheryakov, A.B., Borisova, N.N., Aleksandrova, S. N., and Kuznetsov, V.V. (2002). Can stress-induced CAM provide for performing the developmental program in *Mesembryanthemum crystallinum* plants under long-term salinity? Rus. J. Plant Physiol. 49, 336-343.

Kluge, C., Golldack, D., and Dietz, K. J. (1999). Subunit D of the vacuolar H^+-ATPase of *Arabidopsis thaliana*. Biochem. Biophys. Acta **1419**, 105-110.

Kore-eda, S., Cushman, M.A., Akselrod, I., Bufford, D., Fredrickson, M., Clark, E. and Cushman, J.C. (2004). Transcript profiling of salinity stress responses by large-scale expressed sequence tag analysis in *Mesembryanthemum crystallinum*. Gene **341**, 83-92.

Kuroda, T., Mizushima, T., and Tsuchiya, T. (2005). Physiological roles of three Na^+/H^+ antiporters in the halophilic bacterium *Vibrio parahaemolyticus*. Microb. Immun. **49**, 711–719.

Libik, M., Pater, B., Elliot, S., Slesak, I., and Miszalski, Z. (2004). Malate accumulation in different organis of *Mesembryanthemum crystallinum* L. following age-dependent or salinity-triggered CAM metabolism. Z. Naturforsch. **59c**, 223-228.

Lüttge, U. (1993). The role of crassulacean acid metabolism (CAM) in the adaptation of plants to salinity. New Phytol. **125**, 59-71.

Lüttge, U. (2004). Ecophysiology of Crassulacean Acid Metabolism (CAM). Ann. Bot. (London) **93**, 629-652.

Maathuis, F.J.M., and Sanders, D. (1995). Contrasting roles in ion transport of two K^+-channel types in root cells of *Arabidopsis thaliana*. Planta **197**, 456–464.

Maathuis, F.J.M., and Amtmann, A. (1999). K^+ nutrition and Na^+ toxicity: the basis of cellular K^+/Na^+ ratios. Ann. Bot. (Lond.) **84**, 123–133.

Mahajan, S., and Tuteja, N. (2005). Cold, salinity and drought stresses: an overview. Arch. Biochem. Biophys. **444**, 139-158.

Maresova, L., and Sychrova, H. (2005). Physiological characterization of *Saccharomyces cerevisiae kha1* deletion mutant. Mol. Microbiol. **55**, 588-600.

Mäser, P., Thomine, S., Schroeder, J.I., Ward, J.M., Hirschi, K., Sze, H., Talke, I.N., Amtmann, A., Maathuis, F.J., Sanders, D., Harper, J.F., Tchieu, J., Gribskov, M., Persans, M.W., Salt, D.E., Kim, S.A., and Guerinot, M.L. (2001). Phylogenetic relationships within cation transporter families of *Arabidopsis*. Plant Physiol. **126**, 1646–1667.

Möllering, H. (1974). Metabolite: Substanzen im Citronensäure-Cyclus. L-Malat: Bestimmung mit Malat-Dehydrogenase und Glutamat-Oxalacetat-Transaminase. Methoden der enzymatischen Analyse. Bergmeyer, J.W. (Hrsg.) **2**, 1636-1639.

Nass, R., Cunningham, K.W., and Rao, R. (1997). Intracellular sequestration of sodium by a novel Na^+/H^+ exchanger in yeast is enhanced by mutations in the plasma

membrane H^+-ATPase. Insights into mechanisms of sodium tolerance. J. Biol. Chem. **272**, 26145-26152.

Nass, P., and Rao, R. (1998). Novel localization of a Na^+/H^+ exchanger in the late endosomal compartment of yeast. Implications for vacuole biogenesis. J. Biol. Chem**. 273**, 1054-1060.

Niewiadomska, E., Karpinska, B., Romanowska, E., Slesak, I., and Karpinsi, S. (2004). A salinity-induced C3-CAM transition increases energy conservation in the halophyte Mesembryanthemum crystallinum L. Plant Cell Physiol. **45**, 789-794.

Nobel, P.S. (1996). Physiochemical and environmental plant physiology. 2nd Ed. San Diego, CA. Academic Press.

Nozaki, K., Kuroda, T., Mizushima, T. and Tsuchiya, T. (1998). A new Na^+/H^+ antiporter, NhaD, of *Vibrio parahaemolyticus*. Biochim. Biophys. Acta **1369**, 213–220.

Ottow, E.A., Polle, A., Brosché, M., Kangasjarvi, J., Dibrov, P., Zorb, C., and Teichmann, T. (2005). Molecular characterization of *PeNhaD1*: the first member of the NhaD Na^+/H^+ antiporter family of plant origin. Plant Mol. Biol. **58**, 75-88.

Padan, E., Venturi, M., Gerchman, Y., and Dover, N. (2001). Na^+/H^+ antiporters. Biochim. Biophys. Acta **1505**, 144–157.

Pardo, J.M., Cubero, B., Leidi, E.O., and Quinter, F.J. (2006). Alkali cation exchangers: roles in cellular homeostasis and stress tolerance. J. Exp. Bot. **57**, 1181-1199.

Qiu, Q., Guo, Y., Dietrich, M.A., Schumaker, K.S., and Zhu, J.K. (2002). Regulation of SOS1, a plasma membrane Na^+/H^+ exchanger in *Arabidopsis thaliana*, by SOS2 and SOS3. Proc. Natl. Acad. Sci. USA **99**, 8436–8441

Quintero, F.J., Ohta, M., Shi, H., Zhu, J.K., and Pardo, J.M. (2002). Reconstitution in yeast of the *Arabidopsis* SOS signaling pathway for Na^+ homeostasis. Proc. Natl. Acad. Sci. USA **99**, 9061-9066.

Rengasamy, P. (2006). World salinization with emphasis on Australia. J. Exp. Bot. **57**, 1017-1023.

Ratajczak, R., Richter, J., and Lüttge, U. (1994). Adaptation of the tonoplast V-type H^+-ATPase of *Mesembryanthemum crystallinum* to salt stress, C3-CAM transition and plant age. Plant Cell Env. **17**, 1101-1112.

Rockel, B., Ratajczak, R., Becker, A., and Lüttge, U. (1994). Changed densities and diameters of intra-membrane tonoplast particles of *Mesembryanthemum crystallinum* in correlation with NaCl-induced CAM. J. Plant Physiol. **143**, 318-324

Sanada, Y., Ueda, H., Kuribayashi, K., Andoh, T., Hayashi, F., Tamai, N., and Wada, K. (1995). Novel light-dark change of proline levels in halophyte (*Mesembryanhtemum crystallinum* L.) and glycophytes (*Hordeum vulgare* L. and *Triticum aestivum* L.) leaves and roots under salt stress. Plant Cell Physiol. **36**, 965-970.

Schwacke, R., Schneider, A., van Der Graaff, E., Fischer, K., Catoni, E., Desimone, M., Frommer, W.B., Flugge, U.I., and Kunze, R. (2003). ARAMEMNON, a novel database for Arabidopsis integral membrane proteins. Plant Physiol. **131**, 16-26.

Schwacke, R., Fischer, K., Ketelsen, B., Krupinska, K., and Krause, K. (2007). Comparative survey of plastid and mitochondrial targeting properties of transcription factors in Arabidopsis and rice. Mol. Genet. Genomics **277**, 631-646.

Sentenac, H., Bonneaud, N., Minet, M., Lacroute, F., Salmon, J.M., Gaymard, F., and Grignon, C. (1992). Cloning and expression in yeast of a plant potassium ion transport system. Science **256**, 663–665.

Shi, H., Ishitani, M., Kim, C., and Zhu, J.K. (2000). The *Arabidopsis thaliana* salt tolerance gene SOS1 encodes a putative Na^+/H^+ antiporter. Proc. Natl. Acad. Sci. USA **97**, 6896-6901.

Shi, H., and Zhu, J.K. (2002a). Regulation of expression of the vacuolar Na^+/H^+ antiporter gene AtNHX1 by salt stress and ABA. Plant Mol. Biol. **50**, 543-550.

Shi, H., Quintero, F.J., Pardo, J.M., and Zhu, J.K. (2002b). The putative plasma membrane Na^+/H^+ antiporter SOS1 controls long-distance Na^+ transport in plants. Plant Cell **14**, 465-477.

Su, H., Balders, E., Vera-Estrella, R., Golldack, D., Quigley, F., Zhao, C., Pantoja, O., and Bohnert, H.J. (2003). Expression of the cation transporter McHKT1 in a halophyte. Plant Mol. Biol. **52**, 967-980.

Tester, M., and Davenport, R. (2003). Na^+ tolerance and Na^+ transport in higher plants. Annals Bot. **91**, 503-527.

Thomas, J.C., De Armond, R.L., and Bohnert, H.J. (1992). Influence of NaCl on growth, proline and phosphoenolpyrumate carboxylase levels in *Mesembryanthemum crystallinum* suspension cultures. Plant Physiol. **98**, 626-631

Uozumi, N., Kim, E.J., Rubio, F., Yamaguchi, T., Muto, S., Tsuboi, A., Bakker, E.P., Nakamura, T., and Schroeder, J.I. (2000). The *Arabidopsis* HKT1 gene homolog mediates inward Na^+ currents in *Xenopus laevis* oocytes and Na^+ uptake in *Saccaharomyces cerevisiae*. Plant Physiol. **122**, 1249–1259.

Venema, K., Quintero, F.J., Pardo, J.M., and Donaire, J.P. (2002). The *Arabidopsis* Na^+/H^+ exchanger AtNHX1 catalyzes low affinity Na^+ and K^+ transport in reconstituted liposomes. J. Biol. Chem. **277**, 2413-2418.

Venema, K., Belver, M., Marin-Manzano, M.C., Rodriguez-Rosales, M.P., and Donaire, J.P. (2003). A novel intracellular K^+/H^+ antiporter related to Na^+/H^+ antiporters is important for K^+ ion homeostasis in plants. J. Biol. Chem. **278**, 22453–22459.

Vera-Estrella, R., Barkla, B.J., Bohnert, H.J., and Pantoja, O. (1999). Salt stress in *Mesembryanthemum crystallinum* L. cell suspensions activates adaptive mechanisms similar to those observed in the whole plant. Planta **207**, 426-435

Wang, B., Lüttge, U., and Ratajczak, R. (2001). Effects of salt treatment and osmotic stress on V-ATPase and V-PPase in leaves of the halophyte *Suaeda salsa*. J. Exp. Bot. **52**, 2355-2365.

West, I.C., and Mitchell, P. (1974). Proton/sodium ion antiport in *Escherichia coli*. Biochem. J. **144**, 87-90.

Wild, A. (2003). Soils, land and food: managing the land during the twenty-first century. Cambridge, UK, Cambridge University Press

Winter, K. (1973). Zum Problem der Ausbildung des Crassulaceens/säurestoffwechsels bei *Mesembryanthemum crystallinum* unter NaCl-Einfluss. Planta (Berl.) **109**, 135-145.

Winter, K., Lüttge, U., and Ball, E. (1974). $^{14}CO_2$ dark fixation in the halophytic species *Mesembryanthemum crystallinum*. Biochim. Biophys. Acta **343**, 465-468.

Winter, K., and von Willert, D.J. (1972). NaCl-induzierter crassulace-ensaurestoffwechsel bei *Mesembryanthemum crystallinum*. Zeit. Pflanzen. Bodener. **67**, 166-170.

Wu, S.J., Lei, D., and Zhu, J.K. (1996). SOS1, a genetic locus essential for salt tolerance and potassium acquisition. Plant Cell **8**, 617–627.

Yokoi, S., Quintero, F.J., Cubero, B., Ruiz, M.T., Bressan, R.A., Hasegawa, P.M., and Pardo, J.M. (2002). Differential expression and function of *Arabidopsis thaliana* NHX Na^+/H^+ antiporters in the salt stress response. Plant J. **30**, 529-539.

Zhu, J.K. (2002). Salt and drought stress signal transduction in plants. Annu. Rev. Plant Biol. **53**, 247–273.

Zhu, J.K. (2003). Regulation of ion homeostasis under salt stress. Curr. Opin. Plant Biol. **6**, 441-445.

Zhu, J.K. (2007). In: Encyclopedia of life sciences. John Wiley & Sons, Ltd: Chichester

Eidesstattliche Erklärung

Ich erkläre hiermit an Eides statt, dass ich die vorliegende Dissertation selbstständing und nur mit den angegebenen Hilfsmitteln angefertigt habe.

Milano, den 16 Juni 2008 Unterschrift:

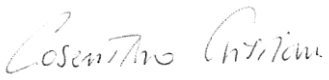

(Dr. Cristian Cosentino)

Curriculum Vitae

Name and surname:	Cristian Cosentino
Date and place of birth:	March 24th 1974, Bollate (Italy)
Nationality:	Italian
E-mail address:	cosentia@gmail.com

University studies and qualifications

May 12th 1999	University of Milan; master degree in Biological Sciences: analysis of a KAT1 K^+ channel mutant from *A. thaliana*
Feb/2001	University of Milan; status qualification as Biologist

Professional experiences

Feb/1998 – May/1999	MSC degree studentship in biology at the University of Milan
Sep/1999 – Sep/2000	Post-lauream internship at IBBA – CNR, Milan: cloning and characterization of zein proteins of *Zea mays*
Oct/2000 – Oct/2001	Compulsory civil service
Nov/2001 – Nov/2004	Fellowship at IBBA – CNR, Milan: epigenetical and functional analysis of zein genes of *Zea mays* and production and sequences management of a *Tuber borchii* cDNA library
Dec/2004 – Nov/2007	PhD fellowship at the TU-Darmstadt: characterization of Na^+/H^+ antiporters in the halophyte *Mesembryanthemum crystallinum*
Dec/2007 – present	Researcher fellowship at the University of Milan: dissection of complex genetic traits by SNP genotyping and genome wide association studies using essential Hypertension as a disease model

Publications

Lazari, B., Cosentino, C., and Viotti, A. (2002) Gene products and structure analysis of wild-type and mutant alleles at the opaque-2 locus of *Zea mays*. Maydica **47**: 253-265

Lazzari, B., Caprera, A., Cosentino, C., Stella, A., Milanesi, L., and Viotti, A. (2007) ESTuber db: an online database for *Tuber borchii* EST sequences. BMC Bioinformatics **8** (Supl. 1): S13